Synthesis and Insertion Behavior of Carbonylhydridonitrosyltris(trimethylphosphine)tungsten(0)

Jürgen Höck, Heiko Jacobsen, Helmut W. Schmalle, Georg R. J. Artus, Thomas Fox, José I. Amor, Frank Bäth, and Heinz Berke*

Anorganisch-chemisches Institut, Universität Zürich, Winterthurerstrasse 190, CH-8057 Zürich, Switzerland

Received September 28, 2000

Two routes for the synthesis of *mer*-W(CO)(H)(NO)$(PMe_3)_3$ (**4**) are described, starting from *mer*-W(Cl)(CO)(NO)$(PMe_3)_3$ (**1**) or the borohydride complex *mer*-W(η^1-BH_4)(CO)(NO)$(PMe_3)_3$ (**3**). The propensity of **4** to undergo insertion reactions has been investigated. **4** reacts with benzaldehyde, propionaldehyde, pivalaldehyde, benzophenone, acetophenone, and acetone to afford the corresponding alkoxide complexes *mer*-W(CO)(NO)$(PMe_3)_3$(OCHR′R″) (R′ = H, R″ = Ph (**5a**); R′ = H, R″ = $CH_2CH_2CH_3$ (**5b**); R′ = H, R″ = $CH_2C(CH_3)_3$ (**5c**); R′ = Ph, R″ = Ph (**5d**); R′ = CH_3, R″ = Ph (**5e**); R′ = CH_3, R″ = CH_3 (**5f**)). Insertion of CO_2 yields the formato-*O* complex *mer*-W(CO)(NO)(OCHO)$(PMe_3)_3$ (**6**). Reaction of **4** with CO leads to immediate loss of PMe_3 and formation of *trans,trans*-W$(CO)_2$(H)(NO)$(PMe_3)_2$. In a reversible way $Fe(CO)_5$ and $Re_2(CO)_{10}$ insert into the W−H bond of **4**, affording the isolable μ-formyl complex *mer*-W(CO)(NO)$(PMe_3)_3$[(μ-OCH)Fe$(CO)_4$] (**7a**) and *mer*-W(CO)(NO)$(PMe_3)_3$[(μ-OCH)-$Re_2(CO)_9$] (**7b**) as an equilibrium constituent. For both reactions equilibrium constants have been derived from VT-NMR measurements and ΔH values were calculated (−46 kJ/mol for **7a** and −26 kJ/mol for **7b**). An accompanying DFT analysis of the W−H bond demonstrated that a higher number of phosphine ligands in a W$(CO)_{4-n}$(H)(NO)$(PMe_3)_n$ series increases the hydridic character of the H ligand and induces a stronger bond polarization. The relative ΔH values for the insertions of the metal carbonyls with $n = 3$ could be reproduced. The calculations also suggest that the main difference in the reactivity of $Fe(CO)_5$ and $Re_2(CO)_{10}$ is not primarily an electronic effect but, rather, is due to steric influence. Compounds **3**, **4**, **6**, and **7a** were structurally characterized by X-ray diffraction studies.

Introduction

Tuning of the ligand sphere allows appropriate adjustment of the reactivity of transition-metal complexes, in particular with respect to their potential application in homogeneous catalysis. For several years our group has studied the ligand sphere influence on the reactivity of metal hydrides.[1] In the context of these investigations the compound *mer*-Mo(CO)(H)(NO)$(PMe_3)_3$ has recently been synthesized.[2] It shows a high propensity for insertion reactions with aldehydes, ketones, imines, CO_2, and metal carbonyls. A remarkable hydridic polarization of the Mo−H bond was noticed, which was apparently caused by the presence of the nitrosyl group[3] and the three strongly σ-donating trimethylphosphine ligands. These Mo investigations were preceded by studies of the tungsten complexes *trans,trans*-W$(CO)_2$(H)(NO)$(PR_3)_2$ with a bis(phosphine) substitution pattern.[1b,4] To evaluate the effect of the metal center and an increasing number of phosphine ligands, we developed access to the tris(phosphine)-substituted *mer*-W(CO)(H)(NO)$(PMe_3)_3$ complex.[5] In this compound the M−H bond was expected to be somewhat stronger than in the mentioned *mer*-Mo(CO)(H)(NO)$(PMe_3)_3$ species,[2] which could influence the overall kinetics and thermodynamics of insertion reactions. In this work we therefore wish to present the preparation of *mer*-W(CO)(H)(NO)$(PMe_3)_3$ and subsequent investigations of its reactivity in insertions with selected aldehydes, ketones, CO_2, and metal carbonyl moieties.

Results and Discussion

Synthesis of *mer*-W(CO)H(NO)$(PMe_3)_3$ (4). Two synthetic routes can be pursued to prepare *mer*-W(CO)-(H)(NO)$(PMe_3)_3$ (**4**), which are depicted in Scheme 1.

(1) (a) Kundel, P.; Berke, H. *J. Organomet. Chem.* **1987**, *335*, 353. (b) Van der Zeijden, A. A. H.; Sontag, C.; Bosch, H. W.; Shklover, V.; Berke, H.; Nanz, D.; von Philipsborn, W. *Helv. Chim. Acta* **1991**, *74*, 1194. (c) Jänicke, M.; Hund, H.-U.; Berke, H. *Chem. Ber.* **1991**, *124*, 719. (d) Van der Zeijden, A. A. H.; Bürgi, T.; Berke, H. *Inorg. Chim. Acta* **1992**, *201*, 131. (e) Gusev, D. G.; Nietlispach, D.; Eremenko, I. L.; Berke, H. *Inorg. Chem.* **1993**, *32*, 3628. (f) Nietlispach, D.; Veghini, D.; Berke, H. *Helv. Chim. Acta* **1994**, *77*, 2197. (g) Nietlispach, D.; Bosch, H. W.; Berke, H. *Chem. Ber.* **1994**, *127*, 2403. (h) Messmer, A.; Jacobsen, H.; Berke, H. *Chem. Eur. J.* **1999**, *5*, 3341. (i) Baur, J.; Jacobsen, H.; Burger, P.; Artus, G.; Berke, H.; Dahlenburg, L. *Eur. J. Inorg. Chem.* **2000**, 1411. (j) Bannwart, E.; Jacobsen, H.; Furno, F.; Berke, H. *Organometallics* **2000**, *19*, 3605. (k) Furno, F.; Fox, T.; Schmalle, H. W.; Berke, H. *Organometallics* **2000**, *19*, 3620.

(2) Liang, F.; Jacobsen, H.; Schmalle, H.; Fox, T.; Berke, H. *Organometallics* **2000**, *19*, 1950.

(3) (a) Berke, H.; Burger, P. *Comments Inorg. Chem.* **1994**, *16*, 279. (b) Bursten, B. E.; Gatter, M. G. *J. Am. Chem. Soc.* **1984**, *106*, 2554.

(4) (a) Van der Zeijden, A. A. H.; Bosch, H. W.; Berke, H. *Organometallics* **1992**, *11*, 563. (b) Van der Zeijden, A. A. H.; Bosch, H. W.; Berke, H. *Organometallics* **1992**, *11*, 2051. (c) Van der Zeijden, A. A. H.; Berke, H. *Helv. Chim. Acta* **1992**, *75*, 513. (d) Van der Zeijden, A. A. H.; Veghini, D.; Berke, H. *Inorg. Chem.* **1992**, *31*, 5106. (e) Shubina, E. S.; Belkova, N. V.; Krylov, A. N.; Vorontsov, E. V.; Epstein, L. M.; Gusev, D. G.; Niedermann, M.; Berke, H. *J. Am. Chem. Soc.* **1996**, *118*, 1105.

(5) (a) Bäth, F. Ph.D. Thesis, University of Zurich, 1998. (b) Höck, J.; Fox, T.; Schmalle, H.; Berke, H. *Chimia* **1999**, *53*, 350.

10.1021/om000838v CCC: \$20.00
Publication on Web 03/14/2001

Scheme 1

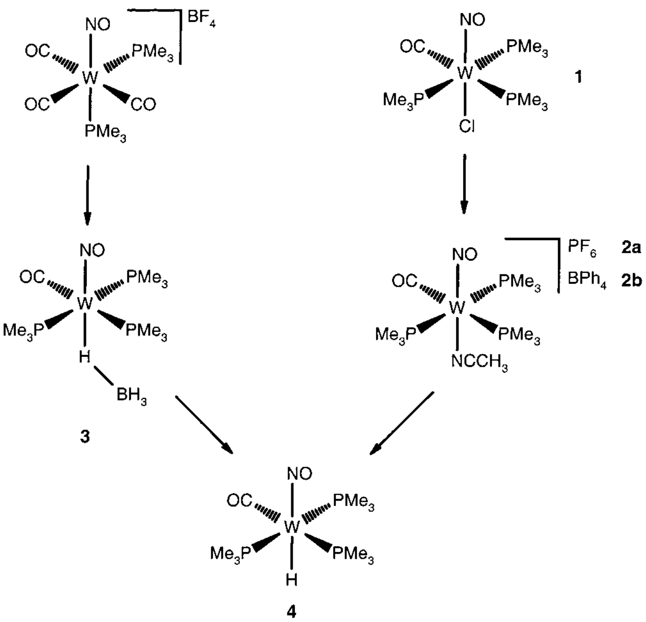

Scheme 2

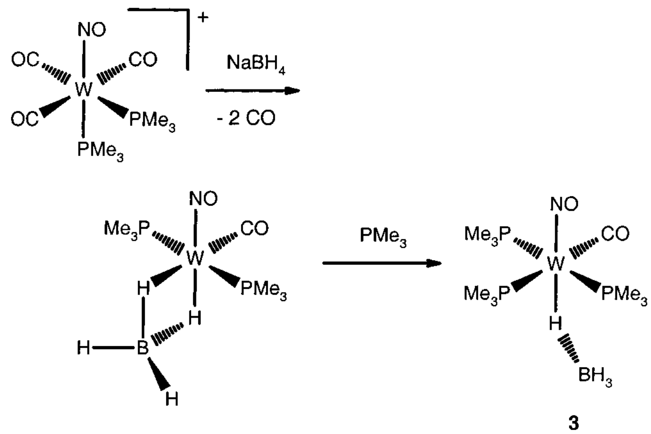

One route starts from *mer*-W(Cl)(CO)(NO)(PMe_3)$_3$ (**1**), which is readily accessible from the reaction of W($AlCl_4$)-(CO)$_4$(NO)[6] with PMe_3 in an autoclave. After workup the product is obtained in 80% yield. The ^{1}H NMR spectrum of **1** in C_6D_6 displays two signals: a doublet at 1.15 ppm arising from the phosphine *trans* to CO and a higher order resonance pattern at 1.36 ppm for the two *trans*-phosphines. The ^{31}P NMR spectrum shows the expected pattern for an AB_2 spin system: a doublet at −26.5 ppm ($^2J_{PP}$ = 20 Hz) and a triplet at −30.8 ppm with the respective ^{183}W satellites.

The removal of the chloride moiety from the tungsten center proved to be troublesome. Most effective were Tl(I) salts with weakly coordinating counterions in coordinating solvents. Therefore, the reaction was carried out with $TlPF_6$ in refluxing CH_3CN. Partial loss of a PMe_3 ligand was observed, which could be suppressed by addition of PMe_3, giving pure [W(CO)($NCCH_3$)(NO)-(PMe_3)$_3$][PF_6] (**2a**). After recrystallization from CH_2Cl_2/Et_2O **2a** was obtained in 67% yield. The ^{1}H NMR spectrum of **2a** in CD_2Cl_2 reveals a resonance at 2.41 ppm for coordinated CH_3CN and, for the three phosphines, a multiplet at 1.67 ppm, together with a doublet at 1.60 ppm.

Attempts to directly convert **2a** to **4** with various hydride transfer reagents (NaBH(OCH_3)$_3$, $NaBH_4$, $LiBH_4$, LiBH(C_2H_5)$_3$, $NaAlH_2$($OCH_2CH_2OCH_3$)$_2$) in various solvents were not successful, and it was suspected that the difficulties originated from an attack of the counterion PF_6^-.[7] Therefore, it was anticipated that an exchange of PF_6^- with BPh_4^- could improve yields of **4** considerably. The ion exchange was achieved by reaction of **2a** with an excess of $NaBPh_4$ in THF. The product [W(CO)-($NCCH_3$)(NO)(PMe_3)$_3$][BPh_4] (**2b**) could be recrystallized from CH_2Cl_2/Et_2O as an orange solid in 79% yield.

Reaction of **2b** with an excess of $NaBH_4$ in THF at 60 °C in the presence of PMe_3 afforded analytically pure **4** within 3 days in 70% yield after recrystallization from pentane at −30 °C. In the IR spectrum in pentane **4** shows a $\tilde{\nu}$(CO) band at 1905 cm^{-1}, a $\tilde{\nu}$(WH) band at 1628 cm^{-1} and a $\tilde{\nu}$(NO) band at 1553 cm^{-1}. In the proton NMR in toluene-d_8 at room temperature the hydride resonance appears at −0.19 ppm with both $^2J_{HP(cis\ to\ CO)}$ and $^2J_{HP(trans\ to\ CO)}$ equal to 27 Hz. When cooled to −50 °C the signal is observed at −0.37 ppm; $^2J_{HP(cis\ to\ CO)}$ becomes 29 Hz and $^2J_{HP(trans\ to\ CO)}$ becomes 24 Hz. This changes the appearance of the resonance, and it is supposed that the changes of the coupling constants with temperature are most likely due to small alterations of the coordination geometry around the tungsten center.

The preparation of **4** via the borohydride complex **3** was developed by starting from the previously reported [W(CO)$_3$(NO)(PMe_3)$_2$][BF_4].[8] This compound was reacted with an excess of $NaBH_4$ at low temperature in THF, and after subsequent addition of PMe_3 *mer*-W(CO)-(HBH_3)(NO)(PMe_3)$_3$ (**3**) was obtained. *mer*-W(CO)(H)-(NO)(PMe_3)$_3$ (**4**) and *cis,cis*- and *trans,trans*-W(CO)$_2$(H)-(NO)(PMe_3)$_2$ were detected as side products. From a pentane solution of this mixture at −30 °C only **3** crystallized to give the analytically pure product in a yield of 27%. Attempts to increase the yield of **3** by concentrating the pentane solution resulted in the crystallization of the concomitant products. Stripping the mother liquor in vacuo, treating the residue with H_3B·THF in THF solution at low temperature, adding PMe_3, and working up as described above gives at least a further 15% of **3**.

Presumably the reaction proceeds via the previously described thermally unstable W(η^2-BH_4)(CO)(NO)-(PMe_3)$_2$,[9] as depicted in Scheme 2. The formation of the side products is very likely due to inter- and/or intramolecular formation of H_3B·PMe_3 and subsequent rearrangements at the tungsten centers.

In the ^{1}H NMR spectrum (toluene-d_8) of **3** the BH_4^- moiety is characterized by a broad signal at −1.40 ppm with a half line width of ca. 290 Hz, indicating an averaging of the bridging and nonbridging protons. No further splitting of this signal could be observed at low temperature. In the ^{31}P NMR spectrum in toluene-d_8 the fine structure of the signals could only be resolved at −40 °C, presumably due to an intramolecular dynamic process or processes, which we were not able to identify.

(6) Seyferth, K.; Taube, R. *J. Organomet. Chem.* **1982**, *229*, 275.
(7) Kundel, P.; Berke, H. *Z. Naturforsch.* **1987**, *42B*, 993.
(8) (a) Honeychuck, R. V.; Hersh, W. H. *Inorg. Chem.* **1987**, *26*, 1826. (b) Hersh, W. H. *J. Am. Chem. Soc.* **1985**, *107*, 4599.
(9) Van der Zeijden, A. A. H.; Shklover, V.; Berke, H. *Inorg. Chem.* **1991**, *30*, 4393.

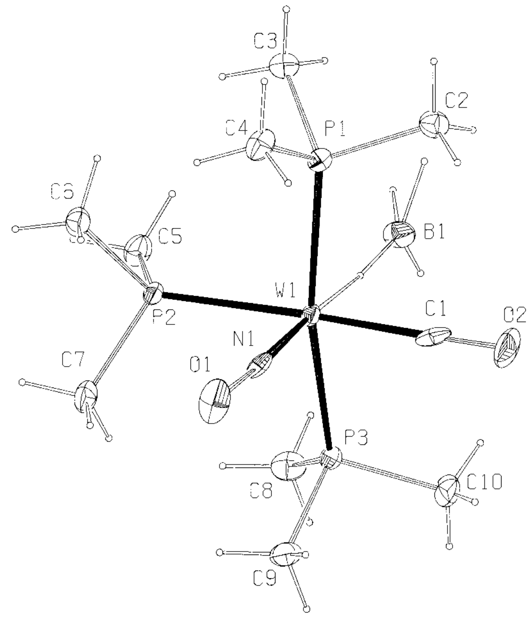

Figure 1. ORTEP plot of the structure of **3**. From the two crystallographically independent molecules, only the complex of W(1) is shown. Displacement ellipsoids are drawn at the 20% probability level. H atoms are represented by circles of arbitrary size.

In solution at ambient temperature **3** is thermally unstable over a prolonged period of time. After 6 days in C_6D_6, considerable decomposition is observed. Among the decomposition products *trans,trans*-W(CO)$_2$(H)(NO)(PMe$_3$)$_2$ and *mer*-W(CO)(H)(NO)(PMe$_3$)$_3$ (**4**) were identified.

Reaction of **3** with 10 equiv of PMe$_3$ in pentane at 45 °C afforded the hydride **4** within 1 h. Evaporation of the solvent, sublimation of the reaction byproduct H$_3$B·PMe$_3$, and subsequent recrystallization from pentane yielded 85% of analytically pure **4**.

Both routes to **4** result in approximately the same overall yield. The route via [W(CO)$_3$(NO)(PMe$_3$)$_2$][BF$_4$] uses one step less, thus being faster. The disadvantage of a more time-consuming synthesis via the *mer*-(W)(Cl)(CO)(NO)(PMe$_3$)$_3$ route is compensated by the possibility of large-scale preparation of **4**. Attempts to scale up the reaction of [W(CO)$_3$(NO)(PMe$_3$)$_2$][BF$_4$] with NaBH$_4$ and PMe$_3$ to afford **4** resulted in a drastic decrease of yield.

X-ray Diffraction Study of *mer*-W(CO)(HBH$_3$)(NO)(PMe$_3$)$_3$ (3) and *mer*-W(CO)(H)(NO)(PMe$_3$)$_3$ (4). Cooling of a concentrated pentane solution of **3** to −30 °C revealed suitable crystals for X-ray diffraction analysis. An ORTEP plot[10] of one molecule of **3** is given in Figure 1. The X-ray data collection and processing parameters are listed in Table 1.

3 is one of only a few examples where a η^1-BH$_4$ complex has been characterized by X-ray diffraction analysis.[2,11] Table 2 shows some selected bond distances and angles for **3**. The W−N distances of 1.764(8) and 1.769(10) Å and the N−O distances of 1.237(10) and 1.238(11) Å of the nitrosyl group of **3** do not reveal significant differences from those of the aforementioned W(η^2-BH$_4$)(CO)(NO)(PMe$_3$)$_2$ species.[9] Hence, similar binding strengths of the nitrosyl groups could be assumed for both compounds. In addition, all the bond distances of **3** turned out to be comparable to those in *mer*-Mo(CO)(HBH$_3$)(NO)(PMe$_3$)$_3$,[2] the lighter congener. The angles W(1)−H(25)−B(1) (146.6°) and W(2)−H(29)−B(2) (138.5°) are significantly distorted from 180°, reflecting secondary interactions with the other ligands in the coordination spheres of the tungsten centers. However, it should be mentioned that the coordinates of the boron-bonded H atoms were fixed and, therefore, it seems inappropriate to discuss the difference between those two angles.

Suitable single crystals for X-ray diffraction analysis of **4** were obtained by cooling of a concentrated solution of **4** in pentane to −30 °C. Because of its air sensitivity the crystal was quickly sealed in a glass capillary and mounted for the measurement at 193 K. A structural

Table 1. Summary of X-ray Diffraction Studies for 3 and 4

	3	4
formula	$C_{10}H_{31}BNO_2P_3W$	$C_{10}H_{28}NO_2P_3W$
color	yellow-orange	orange
cryst dimens (mm)	0.08 × 0.20 × 0.46	0.19 × 0.20 × 0.48
cryst syst	monoclinic	monoclinic
space group (No.)	$P2_1/a$ (14)	$P2_1/n$ (14)
a (Å)	16.0153(10)	9.9941(10)
b (Å)	9.2434(7)	14.4464(14)
c (Å)	26.9274(18)	13.2433(13)
β (deg)	96.900(8)	101.053(12)
V (Å^3)	3957.3(5)	1876.6(3)
Z	8	4
fw	484.93	471.09
d(calcd) (g cm^{-3})	1.628	1.667
abs coeff (mm^{-1})	6.076	6.405
F(000)	1904	920
2θ scan range (deg)	$4.58 < 2\theta < 51.70$	$5.64 < 2\theta < 60.86$
no. of unique data	7385	5271
no. of data obsd ($I > 2\sigma(I)$)	4940	3711
solution method	Patterson	Patterson
no. of params refined	330	159
R1, wR2, all data (%)[a]	6.14, 8.62	4.03, 5.34
R1 (obsd) (%)	3.92	2.46
goodness of fit	1.177	1.009

[a] $R1 = \sum(F_o - F_c)/\sum F_o$; $I > 2\sigma(I)$. $wR2 = \{\sum w(F_o^2 - F_c^2)^2/\sum w(F_o^2)^2\}^{1/2}$.

Table 2. Selected Bond Lengths (Å) and Bond Angles (deg) of Both Molecules of 3

W(1)−N(1)	1.764(8)	W(2)−N(2)	1.769(10)
W(1)−C(1)	1.967(12)	W(2)−C(11)	2.035(10)
W(1)−P(1)	2.487(3)	W(2)−P(4)	2.489(3)
W(1)−P(3)	2.483(3)	W(2)−P(6)	2.476(3)
W(1)−P(2)	2.504(2)	W(2)−P(5)	2.528(2)
W(1)−H(25)	2.06	W(2)−H(29)	1.87
N(1)−O(1)	1.237(10)	N(2)−O(3)	1.238(11)
C(1)−O(2)	1.198(12)	C(11)−O(4)	1.115(11)
P(1)−W(1)−P(3)	166.99(8)	P(4)−W(2)−P(6)	163.93(9)
P(2)−W(1)−C(1)	177.9(3)	P(5)−W(2)−C(11)	174.4(3)
N(1)−W(1)−H(25)	169.6	N(2)−W(2)−H(29)	166.3
W(1)−H(25)−B(1)	146.6	W(2)−H(29)−B(2)	138.5

(10) Spek, A. L. PLATON, PLUTON, An Integrated Tool for the Analysis of the Results of a Single-Crystal Structure Determination. *Acta Crystallogr.* **1990**, *A46*, C34.

(11) (a) Takusagawa, F.; Fumagalli, A.; Koetzle, T. F.; Shore, S. G.; Schmitkons, T.; Fratini, A. V.; Mors, K. W.; Wei, C.-Y.; Bau, R. *J. Am. Chem. Soc* **1981**, *103*, 5165. (b) Ghilardi, C. A.; Midollini, S.; Orlandini, A. *Inorg. Chem.* **1982**, *21*, 4096. (c) Bau, R.; Yuan, H. S. H.; Baker, M. V.; Field, L. D. *Inorg. Chim. Acta* **1986**, *114*, L27. (d) Jensen, J. A.; Girolami, G. S. *J. Am. Chem. Soc.* **1988**, *110*, 4450. (e) Jensen, J. A.; Girolami, G. S. *Inorg. Chem.* **1989**, *28*, 2107. (f) Dionne, M.; Hao, S.; Gambarotta, S. *Can. J. Chem.* **1995**, *73*, 1126. (g) Yoshida, T.; Adachi, T.; Ueda, T.; Akao, H.; Tanaka, T.; Goto, F. *Inorg. Chim. Acta* **1995**, *231*, 95.

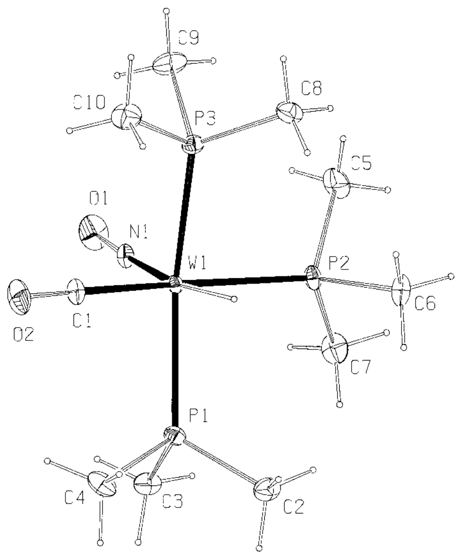

Figure 2. ORTEP plot of the structure of **4**. Displacement ellipsoids are drawn at the 20% probability level. H atoms are represented by circles of arbitrary size.

Table 3. Selected Bond Lengths (Å) and Bond Angles (deg) of 4

W(1)−N(1)	1.820(3)	W(1)−P(2)	2.5010(10)
W(1)−C(1)	1.979(4)	W(1)−H(1)	1.80(4)
W(1)−P(1)	2.4733(9)	N(1)−O(1)	1.218(4)
W(1)−P(3)	2.4574(10)	C(1)−O(2)	1.152(5)
P(1)−W(1)−P(3)	160.02(3)	N(1)−W(1)−H(1)	171.2(11)
P(2)−W(1)−C(1)	170.53(13)		

model of **4** is given in Figure 2; the X-ray data collection and processing parameters are presented in Table 1.

Table 3 shows some selected bond distances and angles for **4**. The distances W(1)−N(1) (1.820(3) Å) and N(1)−O(1) (1.218(4) Å), as well as W(1)−C(1) (1.979(4) Å) and C(1)−O(2) (1.152(5) Å), are very close to the corresponding distances in *mer*-Mo(CO)(H)(NO)(PMe_3)$_3$, thus indicating very similar coordination geometries around the two respective metal centers. Furthermore, the W−H distance (1.80(4) Å) is only slightly shorter than the Mo−H distance. The metal-bound H atom could be located in the difference electron density map and was refined with an isotropic displacement parameter (0.021(9) Å^2). According to the acceptable diffracting volume and the data-to-parameter ratio of 33:1, as well as good reliability factors (*R* values and goodness of fit) as refinement results, the position of the H(1) atom appears to be well-defined.

In comparison to *trans,trans*-W(CO)$_2$(H)(NO)(PMe_3)$_2$, the differences in related bond lengths are very small. Only the C−O distance in **4** is slightly shorter. These geometrical similarities are considered in more detail in the theoretical studies (vide infra).

Insertion Reactions of *mer*-W(CO)(H)(NO)(PMe$_3$)$_3$ (4). In systems such as W(CO)$_2$(H)(NO)(L)$_2$ (L = phosphite, phosphine), hydridic polarization of the M−H bond depends not only on the electronegativity of the metal center,[12] on which the effect of the nitrosyl group has been discussed,[3] but also on the donor capability of L. Hence, the most hydridic tungsten compound was obtained for the strongly donating phosphine series.[1b] We anticipated a further increase of hydride transfer capability by substitution of CO with strongly σ-donating PMe_3 groups. This assumption was probed experimentally by the reactions of **4** with various aldehydes, ketones, CO_2, Fe(CO)$_5$, and Re$_2$(CO)$_{10}$ (Schemes 3 and 4), of which only benzaldehyde is sufficiently activated to react with *trans,trans*-W(CO)$_2$(H)(NO)(PMe_3)$_2$.

The aldehydes gave the fastest insertion reactions with **4**. At ambient temperature in benzene-d_6 the reaction with benzaldehyde (1.5 equiv) was complete after 15 min, with propionaldehyde (1.5 equiv) after 20 min, and with pivalaldehyde (1.2 equiv) after 45 min to yield the alkoxide complexes **5a**−**c**. All of them were isolated as analytically pure orange solids in yields around 75% and are thermally stable at room temperature. However, **5b** decomposed in the reaction solution when too a large excess of propionaldehyde was present and longer reaction times were applied.

Scheme 3

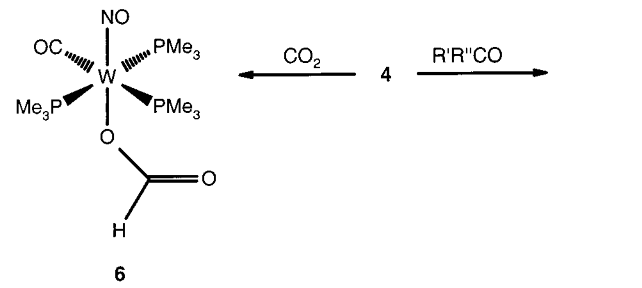

5a: R' = H, R'' = Ph
5b: R' = H, R'' = CH_2CH_3
5c: R' = H, R'' = C(CH_3)$_3$
5d: R' = Ph, R'' = Ph
5e: R' = CH_3, R'' = Ph
5f: R' = CH_3, R'' = CH_3

Scheme 4

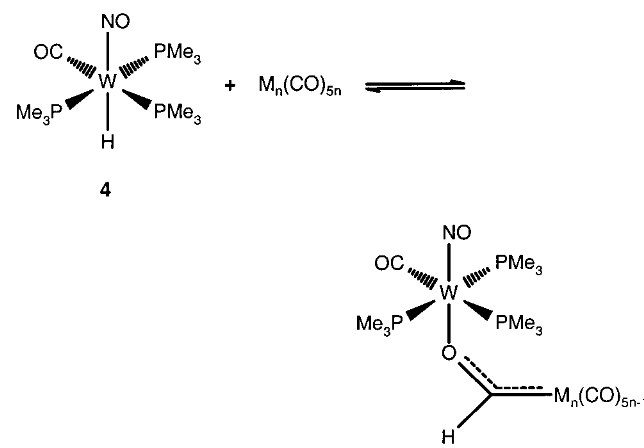

M = Fe, n = 1 **7a**
Re, n = 2 **7b**

(12) (a) Labinger, J. A.; Bercaw, J. E. *Organometallics* **1988**, *7*, 926. (b) Nolan, S. P.; Stern, D.; Marks, T. J. *J. Am. Chem. Soc.* **1989**, *111*, 7844. (c) Marks, T. J. *Bonding Energetics in Organometallic Compounds*; ACS Symposium Series 428; American Chemical Society: Washington, DC, 1990.

The ^1H and $^{13}C\{^1H\}$ NMR spectra in C_6D_6 show characteristic resonances for the $-OCH_2-$ moieties of the products **5a**−**c**. In the ^1H NMR spectrum **5a** displays a singlet for this group at 4.86 ppm, **5b** a triplet at 3.68 ppm ($^3J_{HH} = 6$ Hz), and **5c** a singlet at 3.36 ppm. The corresponding $^{13}C\{^1H\}$ NMR signals appear at 75.8 ppm as a doublet of triplets for **5a** ($^3J_{CP(trans\ to\ CO)} = 8$ Hz, $^3J_{CP(cis\ to\ CO)} = 1$ Hz), a singlet at 75.5 ppm for **5b**, and a doublet of triplets at 85.0 ppm in the case of **5c** ($^3J_{CP(trans\ to\ CO)} = 8$ Hz and $^3J_{CP(cis\ to\ CO)} = 2$ Hz).

We subsequently proceeded to investigate the reactivity of **4** toward ketones. We found that the reaction with benzophenone, acetophenone, and acetone afforded the respective alkoxides **5d**−**f**, though in significantly slower reactions than with the aldehydes. In all cases 4 equiv of ketone and 60 °C had to be used for the reaction to proceed with moderate rates. Using benzophenone, the reaction was complete after 8 h; for acetophenone and acetone it took 4 and 7 days, respectively. **5d**−**f** were all obtained as orange solids in 90%, 73%, and 68% yield, respectively. In the ^1H NMR spectra the $-OCH-$ groups appear as a singlet at 5.46 ppm (toluene-d_8) for **5d**, a quartet at 4.62 ppm (C_6D_6) for **5e** ($^3J_{HH} = 6$ Hz), and a septet at 3.73 ppm (C_6D_6) for **5f** ($^3J_{HH} = 6$ Hz). In the $^{13}C\{^1H\}$ NMR spectrum of **5d** the $-OCH-$ moiety is characterized by a doublet of triplets at 88.1 ppm ($^3J_{CP(trans\ to\ CO)} = 8$ Hz, $^3J_{CP(cis\ to\ CO)} = 1$ Hz). In the $^{13}C\{^1H\}$ NMR spectrum of **5e** this group displays a doublet of triplets at 79.5 ppm ($^3J_{CP(trans\ to\ CO)} = 7$ Hz, $^3J_{CP(cis\ to\ CO)} = 2$ Hz). For **5f** the $^{13}C\{^1H\}$ NMR spectrum shows the corresponding $-OCH-$ signal as a multiplet at 70.9 ppm.

As in the case of *mer*-Mo(CO)(NO)[OCH(CH_3)(Ph)](PMe_3)$_3$[2] the two *trans*-phosphine ligands of **5e** are diastereotopic due to the chiral carbon atom of the $-OCH-$ group and this causes two signals in the ^1H NMR spectrum at 1.39 and at 1.21 ppm. The third phosphine appears at 1.10 ppm. In the $^{31}P\{^1H\}$ NMR spectrum no diastereotopic splitting of the *trans* phosphine signal is observed.

It became apparent that for the rate of formation of **5a**−**f** the electrophilic character of the $C_{carbonyl}$ atom (aldehyde > ketone; benzophenone > acetophenone > acetone) is the decisive factor rather than the steric demands of the substrates. The ease of the insertion reactions of **4** compared to those of *trans,trans*-W(CO)$_2$(H)(NO)(PMe_3)$_2$[2] confirms the expected enhancement in the reactivity by the increase in the number of P-donors. In addition, the resulting compounds **5a**−**f** turned out to be stable with respect to loss of CO despite the *cis*-labilizing effect of the alkoxide groups.[13] This effect causes decomposition of the reaction products in the case of the disubstituted complex *trans,trans*-W(CO)$_2$(H)(NO)(PMe_3)$_2$.[4b]

Encouraged by these results, we additionally investigated the reactivity of **4** toward even more inert types of carbonyl-containing substrates, namely CO_2 and CO.

Formato complexes have been detected as intermediates in the catalytic hydrogenation of CO_2.[14] They are

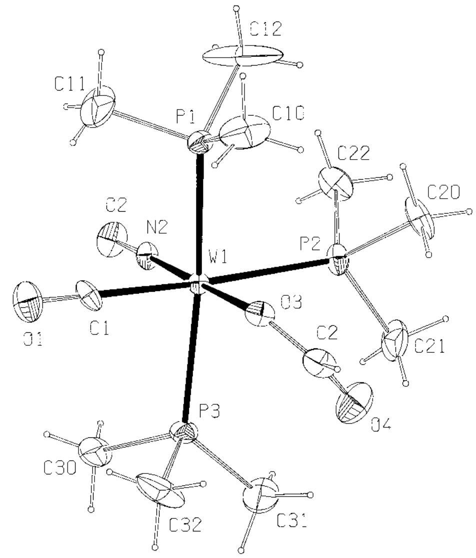

Figure 3. ORTEP plot of the structure of **6**. Displacement ellipsoids are drawn at the 20% probability level. H atoms are represented by circles of arbitrary size.

thus of great interest for an understanding of the mechanism of the hydrogenation of CO_2.

Purging a THF solution of **4** with CO_2 over 50 min indeed resulted in the formation of *mer*-W(CO)(NO)(OCHO)(PMe_3)$_3$ (**6**) (Scheme 3), which could be isolated as an analytically pure orange solid in 30% yield. The spectroscopic data of **6** are very similar to those of the previously reported *mer*-Mo(CO)(NO)(OCHO)(PMe_3)$_3$.[2] In the ^1H NMR spectrum (C_6D_6) the proton of the formato group appears as a multiplet at 8.40 ppm. In the $^{13}C\{^1H\}$ NMR spectrum the $C_{formato}$ atom displays a doublet of triplets at 166.7 ppm. The IR spectrum of **6** in hexane shows an intense $\tilde{\nu}$(NO) band at 1598 cm^{-1} and a $\tilde{\nu}$(OCO) band at 1628 cm^{-1}. In the $\tilde{\nu}$(CO) region two bands are found at 1939 and 1915 cm^{-1}.

Single crystals suitable for X-ray diffraction analysis could be obtained by slow cooling of a concentrated pentane solution of **6** to −30 °C. A structural model of **6** is given in Figure 3. The X-ray data collection and processing parameters are given in Table 4.

There are numerous examples for X-ray diffraction analyses of formato complexes in the literature.[15] Our study of **6** also reveals the existence of a formate group,

(13) (a) Lichtenberger, D. L.; Brown, T. L. *J. Am. Chem. Soc.* **1978**, *100*, 366. (b) Mingos, D. M. P. In *Comprehensive Organometallic Chemistry*; Wilkinson, G., Ed.; Pergamon Press: Oxford, U.K., 1982; Vol. 3, p 24. (c) Macgregor, S. A.; MacQueen, D. *Inorg. Chem.* **1999**, *38*, 4868.

(14) (a) Burgemeister, T.; Kastner, F.; Leitner, W. *Angew. Chem., Int. Ed. Engl.* **1993**, *32*, 739. (b) Leitner, W. *Angew. Chem., Int. Ed. Engl.* **1995**, *34*, 2207. (c) Tsai, J.-C.; Nicholas, K. M. *J. Am. Chem. Soc.* **1992**, *114*, 5117. (d) Darensbourg, D. J.; Ovalles, C.; Pala, M. *J. Am. Chem. Soc.* **1983**, *105*, 5937. (e) Darensbourg, D. J.; Ovalles, C.; Pala, M. *J. Am. Chem. Soc.* **1984**, *106*, 3750. (f) Darensbourg, D. J.; Ovalles, C.; Pala, M. *J. Am. Chem. Soc.* **1987**, *109*, 330. (g) Fu, P.-F.; Fazlur-Rahman, A. K.; Nicholas, K. M. *Organometallics* **1994**, *13*, 413. (h) Yi, C. S.; Lin, N. *Organometallics* **1995**, *14*, 2616.

(15) Selected references: (a) Bianchini, C.; Ghilardi, C. A.; Meli, A.; Midollini, S.; Orlandini, A. *Inorg. Chem.* **1985**, *24*, 924. (b) Fong, L. K.; Fox, J. R.; Cooper, N. J. *Organometallics* **1987**, *6*, 223. (c) Immirzi, A.; Musco, A. *Inorg. Chim. Acta* **1977**, *22*, L35. (d) Darensbourg, D. J.; Fischer, M. B.; Schmidt, R. E., Jr.; Baldwin, B. J. *J. Am. Chem. Soc.* **1981**, *103*, 1297. (e) Guilhem, J.; Pascard, C.; Lehn, J.-M.; Ziessel, R. *J. Chem. Soc., Dalton Trans.* **1989**, 1449. (f) Whittlesey, M. R.; Perutz, R. N.; Moore, M. H. *Organometallics* **1996**, *15*, 5166. (g) Sernau, V.; Huttner, G.; Scherer, J.; Walter, O. *Chem. Ber.* **1996**, *129*, 243. (h) Gibson, D. H.; Ding, Y.; Richardson, J. F.; Mashuta, M. S. *Acta Crystallogr., Sect. C: Cryst. Struct. Commun.* **1996**, *52*, 1614. (i) Grushin, V. V.; Kuznetsov, V. F.; Bensimon, C.; Alper, H. *Organometallics* **1995**, *14*, 3927. (j) Hanna, T. A.; Baranger, A. M.; Bergman, R. G. *J. Am. Chem. Soc.* **1995**, *117*, 11363.

Table 4. Summary of X-ray Diffraction Studies for 6 and 7a

	6	7a
formula	$C_{11}H_{28}NO_4P_3W$	$C_{15}H_{28}FeNO_7P_3W$
color	orange	yellow-orange
cryst dimens (mm)	0.11 × 0.31 × 0.61	0.19 × 0.22 × 0.27
cryst syst	orthorhombic	orthorhombic
space group (No.)	*Pbca* (61)	*Pbca* (61)
a (Å)	8.919(1)	13.6810(8)
b (Å)	15.150(3)	12.6325(5)
c (Å)	29.221(4)	29.4236(12)
V (Å^3)	3948.4(10)	5085.1(4)
Z	8	8
fw	515.12	666.99
d(calcd) (g cm^{-3})	1.73	1.742
abs coeff (mm^{-1})	6.23	5.311
F(000)	2016	2608
2θ scan range (deg)	$5.3 < 2\theta < 58.98$	$4.60 < 2\theta < 61.0$
no. of unique data	5349	5953
no. of data obsd ($I > 1\sigma(I)$)^a	4573	4010
solution method	Patterson	Patterson
no. of params refined	181	262
R1, wR2, all data (%)		5.15, 8.78
R1, wR2, obsd^b (%)	10.54, 6.58	3.74, 8.63
goodness of fit	1.1113	1.059

^{a} $\sigma(I)$ for compound **6**. ^{b} $R1 = \sum(F_o - F_c)/\sum F_o$; $I > 2\sigma(I)$. $wR2 = \{\sum w(F_o^2 - F_c^2)^2/\sum w(F_o^2)^2\}^{1/2}$.

Table 5. Selected Bond Lengths (Å) and Bond Angles (deg) of 6

W(1)−N(2)	1.801(7)	W(1)−O(3)	2.148(7)
W(1)−C(1)	2.009(9)	N(2)−O(2)	1.214(9)
W(1)−P(1)	2.506(2)	C(1)−O(1)	1.12(1)
W(1)−P(3)	2.502(3)	C(2)−O(3)	1.29(1)
W(1)−P(2)	2.549(2)	C(2)−O(4)	1.20(2)
N(2)−W(1)−O(3)	179.0(3)	C(2)−O(3)−W(1)	130.5(8)
P(1)−W(1)−P(3)	168.1(1)	O(3)−C(2)−O(4)	125.6(11)
C(1)−W(1)−P(2)	176.5(3)		

with a distorted-octahedral geometry around the tungsten center. However, due to the poor quality of the crystal and disorder problems with the methyl groups, the bond distances and angles in Table 5 have relatively large standard deviations.

The formation of formyl species from the reaction of CO with a metal−hydride bond has been discussed as a key step in the catalytic process of homogeneous CO hydrogenation.[16] Due to the high bond energy of CO the unique insertion reaction of CO into a metal−hydride bond is not so commonly observed[17] but should be facilitated with increasing hydridic character of the metal hydride. However, despite the high reactivity of **4** in the aforementioned insertion reactions, no formyl species could be found in the reaction with CO. Instead, the apparently more facile substitution of a phosphine ligand by CO occurred, affording *trans,trans*-$W(CO)_2(H)(NO)(PMe_3)_2$ as the sole product. *mer*-Mo(CO)(H)(NO)$(PMe_3)_3$ undergoes a similar CO replacement.[2] Therefore, studies of the insertion behavior of **4** toward CO were tried with metal-bound CO and were accomplished with $Fe(CO)_5$ and $Re_2(CO)_{10}$, affording the μ-formyl complexes *mer*-W(CO)(NO)$(PMe_3)_3$[(μ-OCH)Fe$(CO)_4$] (**7a**) and *mer*-W(CO)(NO)$(PMe_3)_3$[(μ-OCH)$Re_2(CO)_9$] (**7b**) in reversible processes (Scheme 4).

To be able to isolate **7a** from the reaction of **4** with $Fe(CO)_5$ in toluene-d_8 a large excess (15 equiv) of $Fe(CO)_5$ had to be used to shift the equilibrium to the product side. After 1 day, the equilibrium was established (^{1}H NMR monitoring) and the solvent and excess $Fe(CO)_5$ were removed in vacuo. The residue was extracted with a small amount of Et_2O and quickly cooled to −30 °C. At this temperature **7a** crystallized within 6 days and could be isolated as an orange solid in 50% yield.

The spectroscopic data of **7a** resemble closely those of *mer*-Mo(CO)(NO)$(PMe_3)_3$[(μ-OCH)Fe$(CO)_4$].[2] In the ^{1}H NMR spectrum in toluene-d_8 the singlet for H_{formyl} appears at 13.9 ppm. For $[Fe(CO)_4CHO]^-$ Collman et al. have reported a considerable dependence of the C_{formyl} shift in the $^{13}C\{^1H\}$ NMR spectrum on the nature of the solvent and the counterion.[18] Thus, the chemical shift of C_{formyl} of 308.1 ppm for **7a**, which is about 30 ppm downfield from $[Fe(CO)_4CHO]^-$, indicates a strong electron withdrawal from C_{formyl} in the bridging −CHO− group of **7a**. In the IR spectrum of **7a** in Et_2O the $\tilde{\nu}$(CO) bands of the $Fe(CO)_4$ moiety appear at 2035, 1962, and 1927 cm^{-1}. In addition, $\tilde{\nu}$(CO) of the W-coordinated CO is found at 1934 cm^{-1} and ν(NO) at 1611 cm^{-1}.

By slow evaporation of an Et_2O solution of **7a** at −30 °C we obtained crystals suitable for X-ray analysis. A structural model of **7a** is given in Figure 4. The X-ray data collection and processing parameters can be taken from Table 4. For reasons given in the experimental part the bond lengths and angles (Table 6) cannot be discussed in detail; however, the general topology and the μ-binding mode of the −OCH− group is unequivocally established.

In the case of the insertion of $Re_2(CO)_{10}$ into the W−H bond of **4** to afford **7b**, the determined K values are considerably smaller than for **7a** (vide infra). Hence, a large excess of $Re_2(CO)_{10}$ is needed to obtain a reasonable ratio of **7b** to **4**. In the subsequent workup it then turned out to be impossible to separate **7b** from $Re_2(CO)_{10}$. Thus, only a spectroscopic characterization of **7b** can be given. In the ^{1}H NMR spectrum in toluene-d_8 the H_{formyl} resonance appears at 15.05 ppm, which is almost identical with that of *mer*-Mo(CO)(NO)-

(16) (a) Miller, R. L.; Toreki, R.; Wolczanski, P. T.; Van Duyne, G. D.; Roe, D. C. *J. Am. Chem. Soc.* **1993**, *115*, 5570 and references therein. (b) Gladysz, J. A. *Adv. Organomet. Chem*. **1982**, *20*, 1. (c) Burckhardt, U.; Tilley, T. D. *J. Am Chem. Soc.* **1999**, *121*, 6328. (d) Herrmann, W. A. *Angew. Chem., Int. Ed. Engl.* **1982**, *21*, 117. (e) Blackborow, J. R.; Daroda, R. J.; Wilkinson, G. *Coord. Chem. Rev*. **1982**, *43*, 17. (f) Masters, C. *Adv. Organomet. Chem*. **1979**, *17*, 61. (g) Klingler, R. J.; Rathke, J. W. *Prog. Inorg. Chem*. **1991**, *39*, 113. (h) Simpson, M. C.; Cole Hamilton, D. J. *Coord. Chem. Rev*. **1996**, *155*, 163. (i) Süss-Fink, G.; Meister, G. *Adv. Organomet. Chem*. **1993**, *35*, 41. (j) Dombeck, B. P. *Adv. Catal*. **1983**, *32*, 325. (k) Marko, L. *Transition Met. Chem*. **1992**, *17*, 474. (l) Ford, P. C. *Catalytic Activation of Carbon Monoxide*; ACS Symposium Series 152; American Chemical Society: Washington, DC, 1981.

(17) (a) Fagan, P. J.; Moloy, K. G.; Marks, T. J. *J. Am. Chem. Soc.* **1981**, *103*, 6959. (b) Wayland, B. B.; Woods, B. A. *J. Chem. Soc., Chem. Commun*. **1981**, 700. (c) Wei, M. L.; Wayland, B. B. *Organometallics* **1996**, *15*, 4681. (d) Wayland, B. B.; Coffin, V. L.; Sherry, A. E.; Brennen, W. R. *ACS Symp. Ser*. **1990**, *No. 428*, 148. (e) Wayland, B. B.; Sherry, A. E.; Poszmik, G.; Bunn, A. G. *J. Am. Chem. Soc.* **1992**, *114*, 1673. (f) Burckhardt, U.; Tilley, T. D. *J. Am. Chem. Soc.* **1999**, *121*, 6328. (g) Wolczansky, P. T.; Threlkel, R. S.; Bercaw, J. E. *J. Am. Chem. Soc.* **1978**, *101*, 218. (h) Labinger, J. A.; Wong, K. S. *ACS Symp. Ser*. **1981**, *No. 152*, 253. (i) Erker, G.; Schmuck, S.; Hoffmann, U. *J. Am. Chem. Soc.* **1991**, *113*, 2330. (j) Kropp, K.; Skribbe, V.; Erker, G.; Krüger, C. *J. Am. Chem. Soc.* **1983**, *105*, 3353. (k) Fryzuk, M. D.; Mylvaganam, M.; Zaworotko, M. J.; MacGillivray, L. R. *Organometallics* **1996**, *15*, 1134. (l) Rappe, A. K. *J. Am. Chem. Soc.* **1987**, *109*, 5605 and references therein.

(18) Collman, J. P.; Winter, S. R. *J. Am. Chem. Soc.* **1973**, *95*, 4089.

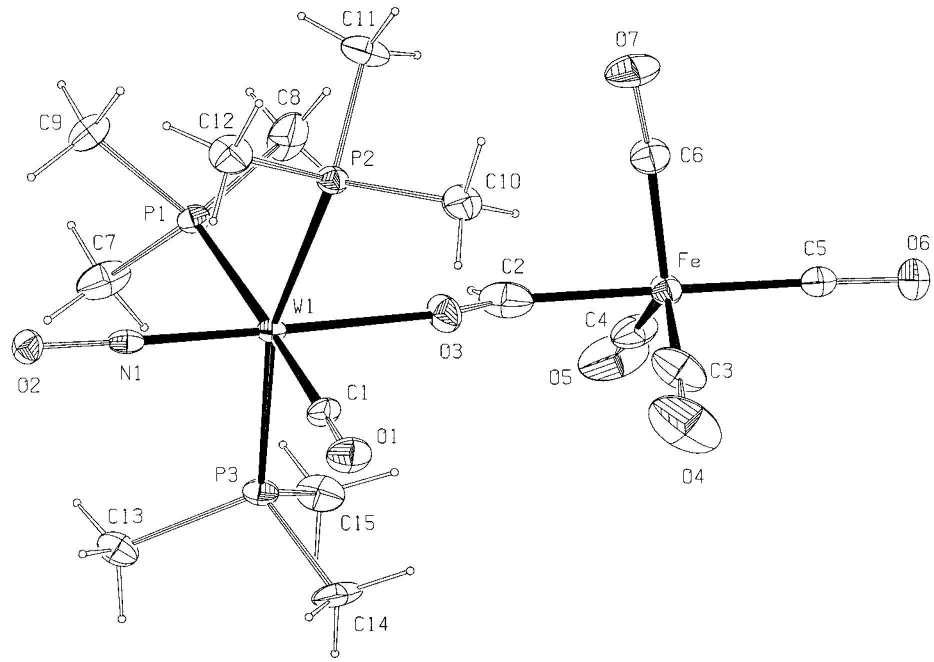

Figure 4. ORTEP plot of the structure of **7a**. Displacement ellipsoids are drawn at the 20% probability level. H atoms are represented by circles of arbitrary size.

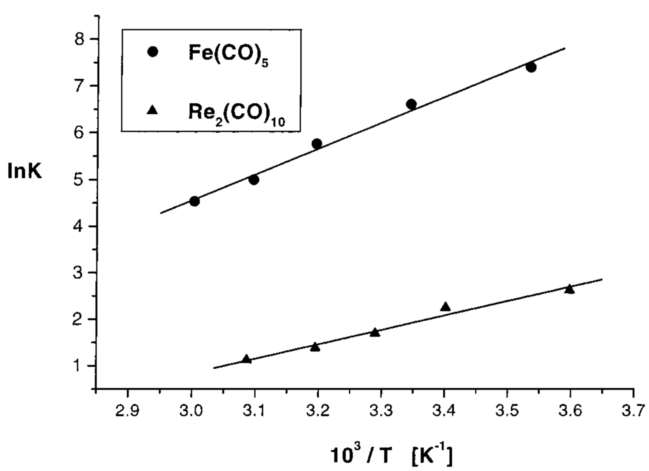

Figure 5. van't Hoff plot for the equilibrium reaction of **4** with $Fe(CO)_5$ and $Re_2(CO)_{10}$ according to Scheme 4.

$(PMe_3)_3[(\mu\text{-}OCH)Re_2(CO)_9]$[2] and close to that of $[Re_2(CO)_9CHO]^-$.[19]

Unlike *mer*-Mo(CO)(H)(NO)$(PMe_3)_3$[2], equilibria of **4** with both $Fe(CO)_5$ and $Re_2(CO)_{10}$ are observable (Scheme 4). For both reactions *K* values were determined by variable-temperature NMR experiments in toluene-d_8. The temperature dependence of *K* allowed for the calculation of ΔH values (see the van't Hoff plot in Figure 5).

For the reaction **4** + $Fe(CO)_5 \rightleftharpoons$ **7a** (where [**7a**] = 0.050 mol/L, prepared by dissolving 20 mg of **7a** in 0.6 mL of toluene-d_8), ΔH was calculated as −46.1 kJ/mol ($\Delta S = -100.4$ eu). **4** + $Re_2(CO)_{10} \rightleftharpoons$ **7b** ([**4**] = 0.068 mol/L, $[Re_2(CO)_{10}]$ = 0.063 mol/L) gave a ΔH value of −26.0 kJ/mol ($\Delta S = -70.0$ eu). Both reactions are moderately exothermic, which indicates a relatively weak W−H bond. Nevertheless, the *K* values for the equilibria of Scheme 4 are smaller than in the case of *mer*-Mo(CO)(H)(NO)$(PMe_3)_3$,[2] suggesting the assumption that the W−H bond is somewhat stronger than the respective Mo−H bond.

(19) Casey, C. P.; Neumann, S. M. *J. Am. Chem. Soc.* **1978**, *100*, 2544.

Table 6. Selected Bond Lengths (Å) and Bond Angles (deg) of 7a

W(1)−N(1)	1.944(6)	W(1)−O(3)	2.323(5)
W(1)−C(1)	1.870(5)	N(1)−O(2)	1.304(7)
W(1)−P(2)	2.5297(14)	C(1)−O(1)	1.064(6)
W(1)−P(3)	2.5162(14)	C(2)−O(3)	1.173(11)
W(1)−P(1)	2.3805(13)	Fe−C(2)	2.053(12)
N(1)−W(1)−O(3)	178.65(16)	C(2)−O(3)−W(1)	151.7(7)
P(2)−W(1)−P(3)	165.09(6)	O(3)−C(2)−Fe	140.8(9)
C(1)−W(1)−P(1)	174.4(2)		

It is noteworthy that both **7a** and **7b** slowly decompose when exposed to higher temperatures (above 60 °C), giving *trans,trans*-W$(CO)_2$(H)(NO)$(PMe_3)_2$ and unidentified complexes of Fe and Re, respectively.

Theoretical Studies. In the last section of our work we present a short analysis of the transition metal hydride bond in compound **4**. In particular, we want to identify how the nature of the transition metal, as well as the number of the phosphine ligands in the coordination sphere around the metal center, might influence the reactivity of the M−H bond. To this end, we compare the optimized geometry of *mer*-W(CO)(H)(NO)$(PMe_3)_3$ (**I**) with those of compounds *trans,trans*-W$(CO)_2$(H)(NO)$(PMe_3)_2$[1b] (**II**) and *mer*-Mo(CO)(H)(NO)$(PMe_3)_3$[2] (**III**). The last two have also been prepared in our laboratories. The calculated structures for molecules **I**−**III** are depicted in Figure 6.

As already observed for the solid-state structures, the M(CO)(H)(NO)$(PMe_3)_3$ (M = W, Mo) systems **I** and **III** display remarkably similar coordination geometries around the central metal and also compound **II** shows only small differences in characteristic bond distances, such as the expected elongation of the W−C bond. It seems that, according to the structural parameters, there is no direct indication for different reactivities of

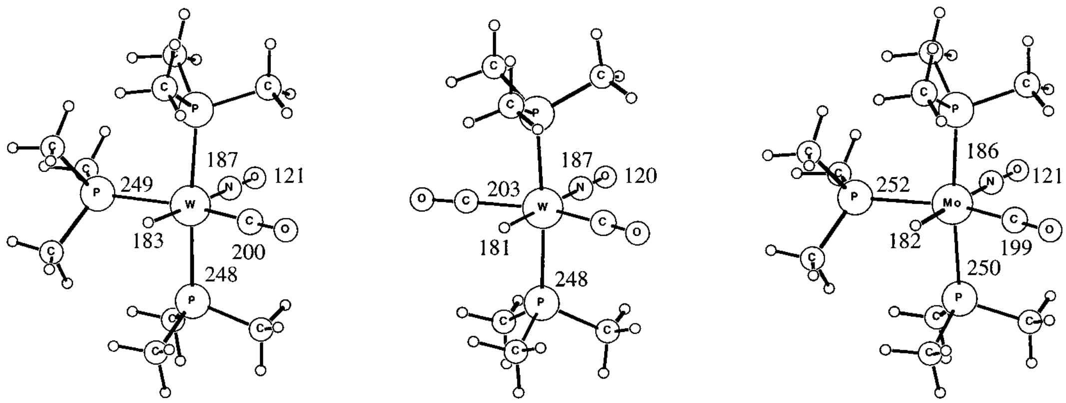

I **II** **III**

Figure 6. Optimized geometries and selected bond distances (in pm) for $M(CO)_{2-n}(H)(NO)(PMe_3)_{2+n}$ compounds **I** (M = W, n = 1), **II** (M = W, n = 0), and **III** (M = Mo, n = 1).

Table 7. Bond Energy Decomposition[a] and Mulliken Charges[b] for $M(CO)_{2-n}(H)(NO)(PMe_3)_{2+n}$ Compounds I (M = W, n = 1), II (M = W, n = 0), and III (M = Mo, n = 1)

	ΔE^0	ΔE_{int}	BE_{snap}	Q(H)
I	−23	−313	336	−0.27
II	−9	−312	321	−0.16
III	−20	−299	319	−0.29

[a] In kJ/mol. [b] In a.u.

these three species, which can, however, be observed experimentally.

To elucidate the salient features of the transition-metal−hydride bond, we have subjected the optimized structures **I**−**III** to a bond analysis.[20] Here, the metal−hydride bond is built up from two fragments, which possess both the right electronic structure and the right geometric structure to form the final molecule. The energy associated with this process is called the bond snapping energy, BE_{snap}, and can be decomposed into a term for steric interaction ΔE^0 and orbital interaction ΔE_{int}:

$$BE_{snap} = -[\Delta E^0 + \Delta E_{int}] \quad (1)$$

Depending on whether Pauli repulsion or electrostatic attraction represents the dominant contribution to ΔE^0, this term is either destabilizing or bonding in nature. Although BE_{snap} values are not defined via the same reaction used for the bond dissociation enthalpies ΔH, they are closely related to bond enthalpy terms, which in turn provide a good description for the bond strength.[21]

The results of this analysis are collected in Table 7. The contribution due to orbital interaction is virtually the same for both tungsten compounds **I** and **II** but about 10 kJ/mol less for the molybdenum compound **III**. Thus, the Mo−H bond is electronically activated compared to the W−H bond by a diminished orbital interaction. For all three compounds, the steric contribution ΔE^0 is stabilizing and therefore dominated by attractive electrostatic interactions. Increasing the number of the phosphorus donors in complex **II** by one leads to a further stabilization of the W−H bond in terms of BE_{snap} by about 15 kJ/mol. This variation is also accompanied by an increase of negative charge at the hydride center, which can be deduced from the Mulliken charges reported in Table 7. We conclude that, by variation of the orbital interaction term, the transition-metal−hydride bond is thermodynamically activated, whereas an enhanced ΔE^0 contribution leads to a more polar M−H bond, inducing a kinetic activation. The former influence can be controlled by variation of the transition-metal center, whereas the latter one can be tuned by the number of phosphorus donors present. Although compound **I** possesses a somewhat stronger W−H bond in terms of the bond snapping energy BE_{snap}, in comparison to compound **II**, we can expect that **I** represents the more reactive compound, due to an enhanced hydridicity, which is in accord with experimental observations. Finally, one has to keep in mind that for thermodynamic considerations not only the strength of the M−H bond but also the stability of the final products has to be taken into account.

The thermodynamics for the insertion reactions of metal carbonyls has also been computationally addressed. We calculate the reaction enthalpies for the processes

$$[W]{-}H + M_n(CO)_{5n} \rightleftharpoons [W]{-}OCH{-}M_n(CO)_{5n-1} \quad (2)$$

$$[W] = W(CO)(NO)(PMe_3)_3$$

as −53 kJ/mol (M = Fe, n = 1) and −34 kJ/mol (M = Re, n = 2). These values are in fair agreement with the ones determined in the NMR equilibrium studies, being higher by about 8 kJ/mol. Of interest is the optimized geometry for [W]-OCH−$Fe(CO)_4$ (**IV**), as shown in Figure 7. In contrast to the solid-state structure, the bridging formyl unit is oriented in a way that the hydrogen atom is pointing toward the carbonyl group of the tungsten moiety.

The W−N distance in **IV** is 3 pm shorter than in **I**, which can be attributed to the *trans* influences of the OR group. We further note that the metal to ligand distance for the phosphorus donor *trans* to the carbonyl group is significantly elongated. This suggests a weakening of the W−P bond, when the insertion product is formed. Indeed, when **7a** is kept in solution at room

(20) Jacobsen, H.; Ziegler, T. *Comments Inorg. Chem.* **1995**, *17*, 301.
(21) Martinho Simões, J. A.; Beauchamp, J. L. *Chem. Rev.* **1990**, *90*, 629.

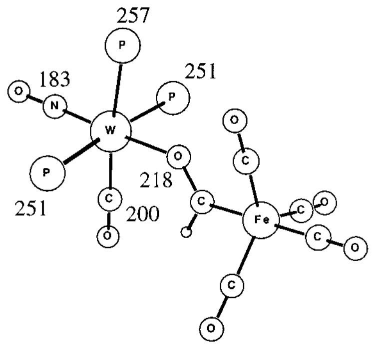

IV

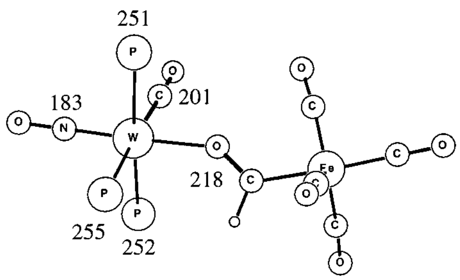

IVa

Figure 7. Optimized geometries (bond distances in pm) for different isomers of the complex $(Me_3P)_3(ON)(OC)W(\mu\text{-}OCH)Fe(CO)_4$. Methyl groups of the PMe_3 ligands are omitted for clarity.

temperature for some time, this particular phosphine ligand is lost from the tungsten fragment, and the μ-formyl unit splits up to form *trans,trans*-$W(CO)_2(H)(NO)(PMe_3)_2$ and presumably $Fe(CO)_4(PMe_3)$.

A geometry for **IV** in which the metal fragments are oriented as in the solid state, which is denoted as **IVa** in Figure 7, is 21 kJ/mol higher in energy and results in a ΔH value of 32 kJ/mol. With this alternative geometry **IVa**, the experimental fact that the insertion of $Fe(CO)_5$ is favored over that of $Re_2(CO)_{10}$ by about 20 kJ/mol cannot be explained. This suggests that **7a** adopts different coordination geometries in the solid state and as a free molecule.

In the adduct $[W]{-}OCH{-}Re_2(CO)_9$ **(V)**, the bridging formyl fragment is oriented in a similar fashion as found for **7a** and for **IVa** and as observed for the related molybdenum compounds.[2] When the calculated enthalpy of formation of **V** is compared with those of **IV** and **IVa**, it becomes clear that the observed difference in the ΔH values for the reaction of **4** with the transition-metal carbonyls $Fe(CO)_5$ and $Re_2(CO)_{10}$ is not governed by differences in the $[W]{-}OCH{-}[M]$ bond strengths but rather by the relative orientation of the metal fragments around the bridging formyl unit. This observation prompted us to reinvestigate the reaction

$$[Mo]{-}H + Fe(CO)_5 \rightleftharpoons [Mo]{-}OCH{-}Fe(CO)_4 \quad (3)$$

$$[Mo] = Mo(CO)(NO)(PMe_3)_3$$

for which we previously reported a calculated ΔH value of -29 kJ/mol. However, the molecular models employed in these calculations were based on the corresponding crystal structures. Reoptimizing the molecular structure of $[Mo]{-}OCH{-}Fe(CO)_4$ **(VI)**, on the basis of the geometry of **IV**, and recalculating ΔH for reaction 3, we obtain a new value of -52 kJ/mol. Adopting a ΔS of 100 eu and taking the initial concentrations of the educts as 0.05 mol/L, this ΔH value leads to a calculated distribution between products and educts of 95% to 5% at room temperature. Under these conditions, one should just be able to observe the equilibrium by NMR spectroscopy. If, however, the calculated, absolute ΔH value is too low by more than 10 kJ/mol, or if the absolute ΔS contribution is overestimated by 30 eu, the remaining educt concentration drops below 1% and cannot be traced by NMR methods any longer.

In our incremental analysis of the bond dissociation energies for the single reactions, which govern the equilibrium (3), we came to the conclusion that the back reaction (3) is kinetically inhibited.[2] The inspection of the related equilibrium between **4** and $Fe(CO)_5$ and **7a** further corroborates this assumption. Starting from **7a**, it takes a time period of 1 day to reach an equilibrium situation. Thus, the reaction of the $[M]{-}OCH{-}Fe(CO)_4$ complex to give $M(CO)(H)(NO)(PMe_3)_3$ and $Fe(CO)_5$ is indeed a slow process.

Conclusions

In this work we have presented two possible routes to the tungsten hydride complex *mer*-$W(CO)(H)(NO)(PMe_3)_3$ (**4**) and investigated its insertion behavior with unsaturated organic molecules and metal carbonyls, the latter forming equilibria.

This investigation has been instructive in several ways: it sets the basis for an understanding of the now proceeding investigations of ionic hydrogenation reactions. It also provides a deeper insight into the possibility of tuning the polarization of the tungsten−hydride bond via the σ-donating properties of phosphines by comparison with the case of *trans,trans*-$W(CO)_2(H)(NO)(PMe_3)_2$.[4] Furthermore, the influence of the metal center on the reactivity could be tested by comparing *mer*-$W(CO)(H)(NO)(PMe_3)_3$ (**4**) with *mer*-$Mo(CO)(H)(NO)(PMe_3)_3$.[2] Finally, the results of those comparisons have been corroborated by DFT calculations.

Experimental Section

General Considerations. All reactions and manipulations were performed under an atmosphere of dry nitrogen using conventional Schlenk techniques or a glovebox. Solvents were dried by standard methods and freshly distilled before use. NMR spectra were recorded on the following spectrometers. Varian Gemini-200 instrument: ^1H at 199.98 MHz, ^{13}C at 50.29 MHz. Varian Gemini-300 instrument: ^1H at 300.08 MHz, ^{13}C at 75.46 MHz, ^{31}P at 121.47 MHz. Bruker DRX-500 instrument: ^1H at 500.13 MHz, ^{13}C at 125.23 MHz, ^{31}P at 202.51 MHz. Chemical shifts $\delta(^1H)$ and $\delta(^{13}C)$ were recorded relative to the solvent and $\delta(^{31}P)$ relative to H_3PO_4. All NMR spectra were recorded at room temperature unless otherwise stated. IR spectra: Biorad FTS-45 instrument. Mass spectra: Finnigan-MAT-8400 spectrometer; FAB spectra in 3-nitrobenzyl alcohol matrix. Elemental analyses: Leco CHN(S)-932 instrument.

Preparation of *mer*-$W(Cl)(CO)(NO)(PMe_3)_3$ (1). *trans*-$W(CO)_4(NO)(\mu\text{-}ClAlCl_3)$ (5.0 g, 10 mmol), prepared according to a literature procedure,[5] was dissolved in THF (150 mL) and transferred into a previously purged steel autoclave via a cannula. PMe_3 (7.4 mL, 71 mmol) in THF (40 mL) was added. The autoclave was heated to 80 °C for 48 h, subsequently cooled to room temperature, purged with nitrogen to remove CO from the reaction mixture, and again heated to 80 °C for another 24 h. After it was cooled to room temperature, the suspension was transferred into a Schlenk via a cannula and then filtered. The solvent was removed in vacuo and the residue extracted with Et_2O until the Et_2O remained colorless. Removal of Et_2O in vacuo gave yellow-orange **1**, which was dissolved in pentane and crystallized at −30 °C. Yield: 3.46 g (80%). IR (cm^{-1}, CH_2Cl_2): 1917 (CO), 1570 (NO). ^1H NMR (200.0 MHz, C_6D_6): δ 1.36 (m, 18H, 2 PMe_3 *trans*), 1.15 (d, $^2J_{HP}$ = 7 Hz, 9H, PMe_3). $^{31}P\{^1H\}$ NMR (121.5 MHz, C_6D_6): δ −26.5 (d with satellites, $^2J_{PP}$ = 20 Hz, $^1J_{PW}$ = 283 Hz, 2 PMe_3 *trans*), −30.8 (t with satellites, $^2J_{PP}$ = 20 Hz; $^1J_{PW}$ = 232 Hz, PMe_3). $^{13}C\{^1H\}$ NMR (50.3 MHz, C_6D_6): δ 227.7 (dt, $^2J_{CP(cis\ to\ CO)}$ = 53 Hz, $^2J_{CP(trans\ to\ CO)}$ = 6 Hz, CO), 18.2 (m, 2 PMe_3 *trans*), 17.5 (dt, $^1J_{CP}$ = 22 Hz, $^3J_{CP}$ = 3 Hz, PMe_3). EI-MS: *m*/*z* 505 [M$^+$], 477 [M$^+$ − CO], 401 [M$^+$ − CO − PMe_3], 325 [M$^+$ − CO − 2 PMe_3]. Anal. Calcd for $C_{10}H_{27}ClNO_2P_3W$: C, 23.67; H, 5.38; N, 2.77. Found: C, 23.91; H, 5.38; N, 2.69.

Preparation of *mer*-[W(CO)(NCCH$_3$)(NO)(PMe$_3$)$_3$][PF$_6$] (2a). To a solid mixture of *mer*-[W(Cl)(CO)(NO)(PMe$_3$)$_3$] (**1**; 3.10 g, 6.13 mmol) and $TlPF_6$ (2.35 g, 6.74 mmol) was added CH_3CN (175 mL) via a cannula. The resulting suspension was refluxed for 12 h, filtered through Celite, and then concentrated. PMe_3 (1 mL, 9.66 mmol) was added to the solution via a syringe. The mixture was then stirred overnight at room temperature and filtered and the solvent removed in vacuo. The residue was dissolved in CH_2Cl_2, Et_2O was added until a precipitate started to form, and **2a** was crystallized at −30 °C. Yield: 2.70 g (67%). IR (cm^{-1}, CH_2Cl_2): 1929 (CO), 1627 (NO). ^1H NMR (200.0 MHz, CD_2Cl_2): δ 2.41 (m, 3H, CH_3CN), 1.67 (m, 18H, 2 PMe_3 *trans*), 1.60 (d, $^2J_{PH}$ = 7 Hz, 9H, PMe_3). $^{31}P\{^1H\}$ NMR (121.5 MHz, CD_2Cl_2): δ −26.4 (d with satellites, $^2J_{PP}$ = 19 Hz, $^1J_{PW}$ = 278 Hz, 2 PMe_3 *trans*), −29.4 (t with satellites, $^2J_{PP}$ = 19 Hz, $^1J_{PW}$ = 240 Hz, PMe_3), −144.0 (sept, $^1J_{PF}$ = 711 Hz, PF_6^-). $^{13}C\{^1H\}$ NMR (50.3 MHz, CD_2Cl_2): δ 225.3 (dt, $^2J_{CP(trans\ to\ CO)}$ = 39 Hz, $^2J_{CP(cis\ to\ CO)}$ = 6 Hz, CO), 125.8 (s, CH_3CN), 18.9 (m, 2 PMe_3 *trans*), 18.2 (dt, $^1J_{CP}$ = 26 Hz, $^3J_{CP}$ = 3 Hz, PMe_3), 3.2 (s, CH_3CN). ^{19}F NMR (282.3 MHz, $CDCl_3$): δ 72.2 (d, $^1J_{PF}$ = 711 Hz, PF_6^-). FAB-MS: *m*/*z* 511 [M$^+$], 470 [M$^+$ − CH_3CN], 442 [M$^+$ − CH_3CN − CO], 366 [M$^+$ − CH_3CN − CO − PMe_3]. Anal. Calcd for $C_{12}H_{30}F_6N_2O_2P_4W$: C, 21.97; H, 4.61; N, 4.27. Found: C, 21.93; H, 4.91; N, 4.10.

Preparation of *mer*-[W(CO)(NCCH$_3$)(NO)(PMe$_3$)$_3$][BPh$_4$] (2b). To a solid mixture of *mer*-[W(CO)(NCCH$_3$)(NO)(PMe$_3$)$_3$]-[PF$_6$] (**2a**; 2.52 g, 3.84 mmol) and $NaBPh_4$ (1.57 g, 4.60 mmol) was added THF (150 mL) via a cannula. The suspension was stirred overnight and filtered and the solvent removed in vacuo. Extraction with CH_2Cl_2 (2 × 200 mL), concentration, and subsequent crystallization by addition of Et_2O and cooling to −30 °C afforded **2b**. The formation of **2b** and the complete consumption of **2a** were confirmed spectroscopically by both the absence of the ^{19}F resonances and the $^{31}P\{^1H\}$ septet and the presence of phenyl resonances in the proton NMR spectrum. Yield: 2.50 g (79%). IR (cm^{-1}, CH_2Cl_2): 1933 (CO), 1636 (NO). ^1H NMR (200.0 MHz, CD_2Cl_2): δ 7.41−7.30 (m, 8H, Ph), 7.08−6.98 (m, 8H, Ph), 6.93−6.83 (m, 4H, Ph). 1.63 (m, 18H, 2 PMe_3 *trans*), 1.51 (d, $^2J_{PH}$ = 7 Hz, 9H, PMe_3), 1.34 (m, 3H, CH_3CN). $^{31}P\{^1H\}$ NMR (121.5 MHz, CD_2Cl_2): δ −27.9 (d with satellites, $^2J_{PP}$ = 19 Hz, $^1J_{PW}$ = 279 Hz, 2 PMe_3 *trans*), −29.7 (t with satellites, $^2J_{PP}$ = 19 Hz, $^1J_{PW}$ = 240 Hz, PMe_3). $^{13}C\{^1H\}$ NMR (125.2 MHz, CD_2Cl_2): δ 224.4 (dt, $^2J_{CP(trans\ to\ CO)}$ = 40 Hz, $^2J_{CP(cis\ to\ CO)}$ = 6 Hz, CO), 164.4 (m, Ph), 136.2 (m, Ph), 126.1 (m, Ph), 125.4 (m, CH_3CN), 122.1 (m, Ph), 18.9 (m, 2 PMe_3 *trans*), 18.3 (m, PMe_3), 1.7 (m, CH_3CN). FAB-MS: *m*/*z* 511 [M$^+$], 470 [M$^+$ − CH_3CN], 442 [M$^+$ − CH_3CN − CO], 366 [M$^+$ − CH_3CN − CO − PMe_3]. Anal. Calcd for $C_{36}H_{50}BN_2O_2P_3W$: C, 52.01; H, 6.07; N, 3.37. Found: C, 52.19; H, 6.33; N, 3.17.

Preparation of *mer*-W(CO)(HBH$_3$)(NO)(PMe$_3$)$_3$ (3). [W(CO)$_3$(NO)(PMe$_3$)$_2$][BF$_4$] (235 mg, 0.440 mmol), which was prepared by a literature procedure,[8] was suspended in THF (350 mL) and cooled to −35 °C. Then $NaBH_4$ (200 mg, 5.3 mmol) was added and the pressure reduced. After 1 h of stirring, PMe_3 (0.1 mL, 0.90 mmol) was added to the now clear solution. The temperature was slowly raised to 10 °C and the solvent removed in vacuo at that temperature. The residue was extracted with pentane, and the orange product **3** crystallized at −30 °C. Yield: 56 mg (27%). Another 36 mg (16%) of **3** could be obtained by the following procedure. The residual pentane solution was evaporated to dryness in vacuo. The resulting oil was dissolved in THF (25 mL) and cooled to −80 °C. $H_3B{\cdot}THF$ in THF solution (0.8 mL, 0.8 mmol) was added and the solution stirred for 1 h. Then PMe_3 (0.1 mL, 0.9 mmol) was added and the solution slowly warmed to room temperature. The solvent was removed in vacuo and $H_3B{\cdot}PMe_3$ removed by sublimation at 35 °C within 3 h. The residue was extracted with pentane and filtered and the resulting solution concentrated. The product crystallized at −30 °C. Overall yield: 92 mg (43%). IR (cm^{-1}, pentane): 2414, 2371 (HB), 1935 (CO), 1607 (NO). ^1H NMR (300.0 MHz, C_6D_6): δ 1.35 (m, 18H, 2 PMe_3 *trans*), 1.10 (d, $^2J_{HP}$ = 7 Hz, 9H, PMe_3), −0.55 to −1.70 (m, 4H, −*H*B*H*$_3$). $^{31}P\{^1H\}$ NMR (121.5 MHz, C_6D_6): δ −28.9 (broad s with satellites, 2 PMe_3 *trans*), −33.7 (broad s with satellites, PMe_3). $^{13}C\{^1H\}$ NMR (125.2 MHz, C_6D_6): δ 227.3 (m, CO), 18.9 (m, 2 PMe_3 *trans*), 18.4 (m, PMe_3). EI-MS: *m*/*z* 409 [M$^+$ − PMe_3], 381 [M$^+$ − PMe_3 − CO], 305 [M$^+$ − 2 PMe_3 − CO]. Anal. Calcd for $C_{10}H_{31}BNO_2P_3W$: C, 24.77; H, 6.44; N, 2.89. Found: C, 24.83; H, 6.22; N, 3.03.

Preparation of *mer*-W(CO)(H)(NO)(PMe$_3$)$_3$ (4). Method A: From *mer*-[W(CO)(NCCH$_3$)(NO)(PMe$_3$)$_3$][BPh$_4$] (2b). To a solid mixture of *mer*-[W(CO)(NCCH$_3$)(NO)(PMe$_3$)$_3$][BPh$_4$] (**2b**; 1.60 g, 1.92 mmol) and $NaBH_4$ (0.51 g, 13.40 mmol) in a Young's tap Schlenk was added THF (100 mL). Then PMe_3 (2 mL, 0.13 mmol) was added via a syringe. The suspension was stirred for 72 h at 60 °C, and then the solvent was slowly removed in vacuo at the same temperature. When the sublimation of $H_3B{\cdot}PMe_3$ was complete, the resulting oil was extracted with Et_2O (2 × 60 mL) and filtered and the solvent removed in vacuo to give a red oil, which was extracted with pentane (2 × 20 mL) in an ultrasonic bath. After filtration the solution was concentrated and left overnight at −30 °C, which gave **4** as a microcrystalline red solid. Yield: 0.63 g (70%).

Method B: From *mer*-W(CO)(HBH$_3$)(NO)(PMe$_3$)$_3$ (3). *mer*-W(CO)(HBH$_3$)(NO)(PMe$_3$)$_3$ (**3**; 90 mg, 0.186 mmol) was dissolved in pentane (40 mL) in a Young's tap Schlenk, and PMe_3 (0.2 mL, 1.80 mmol) was added. After the mixture was heated to 45 °C for 1 h, the solvent was slowly removed in vacuo at the same temperature. When the sublimation of $H_3B{\cdot}PMe_3$ was complete, the resulting oil was extracted with pentane. The solution was concentrated, and the red product **4** crystallized at −30 °C. Yield: 75 mg (85%). IR (cm^{-1}, pentane): 1905 (CO), 1628 (WH), 1553 (NO). ^1H NMR (300.0 MHz, toluene-d_8): δ 1.34 (m, 18H, 2 PMe_3 *trans*), 1.20 (d, $^2J_{HP}$ = 7 Hz, 9H, PMe_3), −0.20 (m, 1H, WH), $^{31}P\{^1H\}$ NMR (121.5 MHz, toluene-d_8): δ −30.4 (d with satellites, $^2J_{PP}$ = 21 Hz, $^1J_{PW}$ = 279 Hz, 2 PMe_3 *trans*), −36.7 (t with satellites, $^2J_{PP}$ = 21 Hz, $^1J_{PW}$ = 233 Hz, PMe_3). $^{13}C\{^1H\}$ NMR (50.3 MHz, toluene-d_8): δ 234.4 (m, CO), 22.7 (m, 2 PMe_3 *trans*), 22.0 (dt, $^1J_{CP}$ = 23 Hz, $^3J_{CP}$ = 3 Hz, PMe_3). FAB-MS: *m*/*z* 470 [M$^+$]. Anal. Calcd for $C_{10}H_{28}NO_2P_3W$: C, 25.50; H, 5.99; N, 2.97. Found: C, 25.72; H, 5.65; N, 2.99.

Preparation of *mer*-W(CO)(NO)(OCH$_2$Ph)(PMe$_3$)$_3$ (5a). *mer*-W(CO)(H)(NO)(PMe$_3$)$_3$ (**4**; 21 mg, 0.044 mmol) was dissolved in C_6D_6 (1 mL), and benzaldehyde (9 μL, 0.066 mmol) was added. After 15 min the reaction was complete (^1H NMR monitoring) and the solvent removed in vacuo. The residue was recrystallized from pentane (0.5 mL) at −30 °C to give orange **5a**. Yield: 20 mg (78%). IR (cm^{-1}, pentane): 1904 (CO), 1572 (NO). ^1H NMR (300.0 MHz, C_6D_6): δ 7.40−7.32 (m, 2H, Ph), 7.29−7.23 (m, 2H, Ph), 7.13−7.07 (m, 1H, Ph), 4.86 (s, 2H, $-CH_2O-$), 1.29 (m, 18H, 2 PMe_3 *trans*), 1.13 (d, $^2J_{HP} = 7$ Hz, 9H, PMe_3). $^{31}P\{^1H\}$ NMR (121.5 MHz, C_6D_6): δ −25.1 to −25.3 (m with satellites, 2 PMe_3 *trans*), −26.0 to −26.3 (m with satellites, PMe_3). $^{13}C\{^1H\}$ NMR (125.2 MHz, C_6D_6): δ 229.2 (dt, $^2J_{CP(cis\ to\ CO)} = 6$ Hz, $^2J_{CP(trans\ to\ CO)} = 54$ Hz, CO), 149.4 (s, Ph), 127.7 (s, Ph), 125.7 (s, Ph), 125.5 (s, Ph), 75.8 (dt, $^3J_{CP(cis\ to\ CO)} = 1$ Hz, $^3J_{CP(trans\ to\ CO)} = 8$ Hz, $-CH_2O-$), 18.2 (m, 2 PMe_3 *trans*), 17.2 (dt, $^1J_{CP} = 20$ Hz, $^3J_{CP} = 3$ Hz, PMe_3). EI-MS: *m/z* 577 [M^+], 549 [$M^+ - CO$], 501 [$M^+ - PMe_3$], 473 [$M^+ - CO - PMe_3$]. Anal. Calcd for $C_{17}H_{34}NO_3P_3W$: C, 35.37; H, 5.94; N, 2.43. Found: C, 35.12; H, 5.54; N, 2.35.

Preparation of *mer*-W(CO)(NO)($OCH_2CH_2CH_3$)(PMe_3)$_3$ (5b). *mer*-W(CO)(H)(NO)(PMe_3)$_3$ (**4**; 14 mg, 0.030 mmol) was dissolved in C_6D_6 (1 mL), and propionaldehyde (3.3 μL, 0.045 mmol) was added. After 20 min the reaction was complete (^1H NMR monitoring) and the solvent removed in vacuo. Longer reaction times and a larger excess of the aldehyde lead to decomposition of the product. The orange residue was recrystallized from pentane (0.5 mL) at −30 °C to give **5b**. Yield: 12 mg (76%). IR (cm^{-1}, pentane): 1906 (CO), 1567 (NO). ^1H NMR (300.0 MHz, C_6D_6): δ 3.68 (t, $^3J_{HH} = 6$ Hz, 2H, $-OCH_2-$), 1.46−1.36 (m, 2H, $-OCH_2-CH_2^-$), 1.35 (m, 18H, 2 PMe_3 *trans*), 1.10 (d, $^2J_{HP} = 6$ Hz, 9H, PMe_3), 0.94 (t, $^3J_{HH} = 7$ Hz, 3H, $-CH_3$). $^{31}P\{^1H\}$ NMR (121.5 MHz, C_6D_6): δ −25.5 to −25.8 (m with satellites, 2 PMe_3 *trans*), −26.4 to −26.7 (m with satellites, PMe_3). $^{13}C\{^1H\}$ NMR (125.2 MHz, C_6D_6): δ 229.7 (m, CO), 75.5 (s, $-OCH_2-$), 30.6 (s, $-OCH_2CH_2-$), 18.4 (m, 2 PMe_3 *trans*), 17.2 (dt, $^1J_{CP} = 20$ Hz, $^3J_{CP} = 3$ Hz, PMe_3), 11.2 (s, $-CH_3$). EI-MS: *m/z* 529 [M^+], 501 [$M^+ - CO$], 425 [$M^+ - CO - PMe_3$], 382 [$M^+ - CO - PMe_3 - CH_2CH_2CH_3$]. Anal. Calcd for $C_{13}H_{34}NO_3P_3W$: C, 29.51; H, 6.48; N, 2.65. Found: C, 29.87; H, 6.30; N, 2.70.

Preparation of *mer*-W(CO)(NO)[$OCH_2C(CH_3)_3$](PMe_3)$_3$ (5c). *mer*-W(CO)(H)(NO)(PMe_3)$_3$ (**4**; 22 mg, 0.046 mmol) was dissolved in C_6D_6 (1 mL) and pivalaldehyde (5.9 μL, 0.054 mmol) was added. After 45 min the reaction was complete (^1H NMR monitoring) and the solvent removed in vacuo. The residue was extracted with pentane (0.5 mL), filtered and crystallized at −30 °C to give orange **5c**. Yield: 17.3 mg (67%). IR (cm^{-1}, pentane): 1908 (CO), 1569 (NO). ^1H NMR (300.0 MHz, C_6D_6): δ 3.36 (s, 2H, $-OCH_2-$), 1.36 (m, 18H, 2 PMe_3 *trans*), 1.12 (d, $^2J_{HP} = 6$ Hz, 9H, PMe_3), 0.90 (s, 9H, $-CH_3$). $^{31}P\{^1H\}$ NMR (121.5 MHz, C_6D_6): δ −25.9 to −26.9 (m with satellites, 3 PMe_3). $^{13}C\{^1H\}$ NMR (125.2 MHz, C_6D_6): δ 229.3 (m, CO), 85.0 (dt, $^3J_{CP(trans\ to\ CO)} = 8$ Hz, $^3J_{CP(cis\ to\ CO)} = 2$ Hz, $-OCH_2-$), 35.6 (s, CMe_3), 27.3 (s, $-CH_3$),18.5 (m, 2 PMe_3 *trans*), 17.3 (dt, $^1J_{CP} = 20$ Hz, $^3J_{CP} = 3$ Hz, PMe_3). EI-MS: *m/z* 557 [M^+], 529 [$M^+ - CO$], 481 [$M^+ - PMe_3$], 453 [$M^+ - CO - PMe_3$]. Anal. Calcd for $C_{15}H_{38}NO_3P_3W$: C, 32.33; H, 6.87; N, 2.51. Found: 32.67; H, 6.43; N, 2.52.

Preparation of *mer*-W(CO)(NO)($OCHPh_2$)(PMe_3)$_3$ (5d). *mer*-W(CO)(H)(NO)(PMe_3)$_3$ (**4**; 15 mg, 0.032 mmol) was dissolved in toluene-d_8 (1 mL), and benzophenone (24 mg, 0.128 mmol) was added. After the mixture was heated to 60 °C for 8 h, the reaction was complete (^1H NMR monitoring) and the solvent removed in vacuo. The residue was recrystallized from pentane (0.7 mL) at −30 °C to give orange **5d**. Yield: 19 mg (90%). IR (cm^{-1}, CH_2Cl_2): 1895 (CO), 1539 (NO). ^1H NMR (300.0 MHz, toluene-d_8): δ 7.90−6.80 (m, 10H, Ph), 5.46 (s, 1H, $-OCHPh_2$), 1.20 (d, $^2J_{HP} = 7$ Hz, 9H, PMe_3), 1.12 (m, 18H, 2 PMe_3 *trans*). $^{31}P\{^1H\}$ NMR (121.5 MHz, toluene-d_8): δ −25.7 (t with satellites, $^2J_{PP} = 19$ Hz, $^1J_{PW} = 242$ Hz, PMe_3), −27.5 (d with satellites, $^2J_{PP} = 19$ Hz, $^1J_{PW} = 287$ Hz, 2 PMe_3 *trans*). $^{13}C\{^1H\}$ NMR (75.5 MHz, toluene-d_8): δ 229.0 (dt, $^2J_{CP(trans\ to\ CO)} = 55$ Hz, $^2J_{CP(cis\ to\ CO)} = 6$ Hz, CO), 151.7 (s, Ph), 127.9 (s, Ph), 126.9 (s, Ph), 126.0 (s, Ph), 88.1 (dt, $^3J_{CP(trans\ to\ CO)} = 8$ Hz, $^3J_{CP(cis\ to\ CO)} = 1$ Hz, $-OCHPh_2$), 18.5 (m, 2 PMe_3 *trans*), 17.7 (m, PMe_3). EI-MS: *m/z* 653 [M^+], 625 [$M^+ - CO$], 577 [$M^+ - PMe_3$], 549 [$M^+ - CO - PMe_3$]. Anal. Calcd for $C_{23}H_{38}NO_3P_3W$: C, 42.28; H, 5.86; N, 2.14. Found: C, 42.68; H, 5.81; N, 2.15.

Preparation of *mer*-W(CO)(NO)[$OCH(CH_3)(Ph)$](PMe_3)$_3$ (5e). *mer*-W(CO)(H)(NO)(PMe_3)$_3$ (**4**; 26 mg, 0.055 mmol) was dissolved in C_6D_6 (1 mL), and acetophenone (26 μL, 0.221 mmol) was added. The solution was heated to 60 °C, and the reaction was complete after 4 days (^1H NMR monitoring). The solvent was removed in vacuo, and the residue recrystallized from pentane (0.6 mL) at −30 °C to give orange **5e**. Yield: 24 mg (73%). IR (cm^{-1}, pentane): 1906 (CO), 1568 (NO). ^1H NMR (300.0 MHz, C_6D_6): δ 7.32−7.19 (m, 4H, Ph), 7.10−7.05 (m, 1H, Ph), 4.62 (q, $^3J_{HH} = 6$ Hz, 1H, $-OCHMePh$), 1.39 (m, 9H, PMe_3 *cis* to CO), 1.29 (d, $^3J_{HH} = 6$ Hz, 3H, $-CH_3$), 1.21 (m, 9H, PMe_3 *cis* to CO), 1.10 (d, $^2J_{HP} = 6$ Hz, PMe_3 *trans* to CO). $^{31}P\{^1H\}$ NMR (121.5 MHz, C_6D_6): δ −27.2 to −27.5 (m with satellites, PMe_3), −27.9 to −28.1 (m with satellites, 2 PMe_3 *trans*). $^{13}C\{^1H\}$ NMR (75.5 MHz, C_6D_6): δ 229.6 (m, CO), 153.5 (s, Ph), 127.9 (s, Ph), 126.0 (s, Ph), 125.9 (s, Ph), 79.5 (dt, $^3J_{CP(trans\ to\ CO)} = 7$ Hz, $^3J_{CP(cis\ to\ CO)} = 2$ Hz, $-OCHMePh$), 30.0 (s, $-CH_3$), 18.6−18.1 (m, 2 PMe_3 *trans*), 17.3−16.9 (m, PMe_3). EI-MS: *m/z* 591 [M^+], 563 [$M^+ - CO$], 487 [$M^+ - CO - PMe_3$], 411 [$M^+ - CO - 2\ PMe_3$]. Anal. Calcd for $C_{18}H_{36}NO_3P_3W$: C, 36.57; H, 6.14; N, 2.37. Found: C, 36.43; H, 6.27; N, 2.39.

Preparation of *mer*-W(CO)(NO)[$OCH(CH_3)_2$](PMe_3)$_3$ (5f). *mer*-W(CO)(H)(NO)(PMe_3)$_3$ (**4**; 28 mg, 0.058 mmol) was dissolved in C_6D_6 (0.8 mL), and then acetone (17 μL, 0.232 mmol) was added. The solution was heated to 60 °C, and the reaction was complete after 7 days (^1H NMR monitoring). The solvent was removed in vacuo and the residue recrystallized from pentane (0.5 mL) at −30 °C to give **5f** as an orange solid. Yield: 21 mg (68%). IR (cm^{-1}, pentane): 1905 (CO), 1565 (NO). ^1H NMR (300.0 MHz, C_6D_6): δ 3.73 (sept, $^3J_{HH} = 6$ Hz, 1H, $-OCHMe_2$), 1.37 (m, 18H, 2 PMe_3 *trans*), 1.09 (d, $^2J_{HP} = 6$ Hz, 9H, PMe_3), 1.05 (d, $^3J_{HH} = 6$ Hz, 6H, $-CH_3$). $^{31}P\{^1H\}$ NMR (121.5 MHz, C_6D_6): δ −27.6 to −28.2 (m with satellites, 3 PMe_3). $^{13}C\{^1H\}$ NMR (125.2 MHz, C_6D_6): δ 229.4 (m, CO), 70.9 (m, $-OCHMe_2$), 28.8 (s, $-CH_3$), 18.3 (m, 2 PMe_3 *trans*), 16.8 (m, PMe_3). EI-MS: *m/z* 529 [M^+], 501 [$M^+ - CO$], 425 [$M^+ - CO - PMe_3$], 349 [$M^+ - CO - 2\ PMe_3$]. Anal. Calcd for $C_{13}H_{34}NO_3P_3W$: C, 29.51; H, 6.48; N, 2.65. Found: C, 29.45; H, 6.05; N, 2.68.

Preparation of *mer*-W(CO)(NO)(OCHO)(PMe_3)$_3$ (6). A solution of *mer*-W(CO)(H)(NO)(PMe_3)$_3$ (**4**; 100 mg, 0.210 mmol) in THF (10 mL) was purged with CO_2 over a period of 50 min. The solvent was removed in vacuo and the residue extracted with Et_2O (5 mL). Evaporation of the solvent in vacuo gave **6** as an orange solid. Yield: 32 mg (30%). IR (cm^{-1}, hexane): 1939 (CO), 1915 (CO), 1628 (OCO), 1598 (NO). ^1H NMR (200.0 MHz, C_6D_6): δ 8.40 (m, 1H, $-OCOH$), 1.33 (m, 18H, 2 PMe_3), 1.17 (d, $^2J_{HP} = 7$ Hz, 9H, PMe_3). $^{31}P\{^1H\}$ NMR (121.5 MHz, C_6D_6): δ −22.1 (d with satellites, $^2J_{PP} = 20$ Hz, $^1J_{PW} = 298$ Hz, 2 PMe_3), −26.1 (t with satellites, $^2J_{PP} = 20$ Hz, $^1J_{PW} = 242$ Hz; PMe_3). $^{13}C\{^1H\}$ NMR (50.3 MHz, C_6D_6): δ 228.1 (dt, $^2J_{CP(trans\ to\ CO)} = 52$ Hz, $^2J_{CP(cis\ to\ CO)} = 6$ Hz, CO), 166.7 (dt, $^3J_{CP(trans\ to\ CO)} = 4$ Hz, $^3J_{CP(cis\ to\ CO)} = 3$ Hz, $-OCOH$), 18.6 (m, 2 PMe_3 *trans*), 18.2 (dt, $^1J_{CP} = 22$ Hz, $^3J_{CP} = 3$ Hz, PMe_3). FAB-MS: *m/z* 487 [$M^+ - CO$], 470 [$M^+ - OCHO$], 439 [$M^+ - PMe_3$], 411 [$M^+ - CO - PMe_3$]. Anal. Calcd for $C_{11}H_{28}NO_4P_3W$: C, 25.65; H, 5.48; N, 2.72. Found: C, 25.74; H, 5.20; N, 2.70.

Preparation of *mer*-W(CO)(NO)(PMe_3)$_3$[(μ-OCH)Fe(CO)$_4$] (7a). *mer*-W(CO)(H)(NO)(PMe_3)$_3$ **4** (20 mg, 0.042 mmol) was dissolved in toluene-d_8 (1 mL) and an excess of $Fe(CO)_5$ was added (ca. 15 equiv). After 1 d there was no further change in the ratio of **4** to **7a**, as monitored by $^{31}P\{^1H\}$ NMR spectroscopy. After the solvent was removed in vacuo the residue was extracted with Et_2O (2 mL) and filtered. When the Et_2O was allowed to evaporate slowly at −30 °C crystals of **7a** formed after 6 d. Yield: 14 mg (50%). IR (cm^{-1}, Et_2O): 2035 (Fe−CO), 1962 (Fe−CO), 1934 (W−CO), 1927 (Fe−CO), 1611 (NO). ^1H NMR (300.0 MHz, toluene-d_8): δ 13.9 (s, $-CHO-$), 1.10−1.07 (m, 3 PMe_3). $^{31}P\{^1H\}$ NMR (121.5 MHz, toluene-d_8): δ −21.6 to 21.8 (m with satellites, 2 PMe_3 *trans*), −22.8 − −23.3 (m with satellites, PMe_3). $^{13}C\{^1H\}$ NMR (125.2 MHz, toluene-d_8): δ 308.1 (m, −OCH−), 227.3 (dt, $^2J_{CP(trans\ to\ CO)}$ = 46 Hz, $^2J_{CP(cis\ to\ CO)}$ = 6 Hz, CO), 217.7 (s, −Fe(CO)$_4$), 17.9 (m, 2 PMe$_3$ *trans*), 17.4 (m, PMe3). FAB-MS: *m*/*z* 667 [M$^+$], 639 [M$^+$ − CO]. Anal. Calcd for $C_{15}H_{28}FeNO_7P_3W$: C, 27.01; H, 4.23; N, 2.10. Found: C, 27.33; H, 4.06; N, 2.14.

Attempt To Isolate *mer*-W(CO)(NO)(PMe$_3$)$_3$[(μ-OCH)-Re$_2$(CO)$_9$] (7b). *mer*-W(CO)(H)(NO)(PMe$_3$)$_3$ (**4**; 23 mg, 0.048 mmol) was dissolved in toluene-d_8 (2 mL), and Re$_2$(CO)$_{10}$ (144 mg, 0.220 mmol) was added. After 8 days an equilibrium was attained (^{31}P NMR monitoring). The solution was slowly cooled to −30 °C. After 5 days a mixture of Re$_2$(CO)$_{10}$ and **7b** crystallized. Extraction with Et$_2$O and cooling also afforded the same mixture. Separation of **7b** and Re$_2$(CO)$_{10}$ has not yet been achieved so far.

Computational Details. The density functional calculations utilized the ADF program package, release 1999.01 and 2000.01.[22] Energies and geometries were evaluated by using the local exchange-correlation potential of Vosko and coworkers,[23] augmented in a self-consistent manner with gradient corrections for exchange and correlation, due to Becke[24] and Perdew,[25] respectively. For the *n*s, *n*p, *n*d, and (n + 1)s shells on the transition metals and for the hydride, a triple-ζ STO basis augmented by one (n + 1)p function was employed (ADF database IV). The valence shell of the remaining main-group elements was described with a double-ζ STO basis and one d-STO polarization function (ADF database III). In reactions involving the iron or rhenium carbonyl fragments, methyl groups were described using a double-ζ STO basis (ADF database II). Relativistic effects were included using a quasi-relativistic approach.[26] Corrections for zero point energy (ZPE) and for solvation effects were applied as described before.[2]

X-ray Crystal Structure Analyses on 3, 4, 6, and 7a. X-ray diffraction data were collected at 193(1) K for **3** and **4** and 183(1) K for **7a** using an imaging plate detector system (Stoe IPDS) with graphite-monochromated Mo Kα radiation. A total of 222, 143, and 270 images were exposed at constant times of 1.50, 1.60, and 1.80 min/image for **3**, **4**, and **7a**, respectively. The crystal-to-image distances were set to 70, 50, and 60 mm (θ_{max} = 25.85, 30.43, and 30.50°). ϕ rotation (**3** and **4**) or oscillation modes (**7a**) were used for the ϕ increments of 0.9, 1.4, and 0.7° per exposure in each case. Total exposure times for **3**, **4**, and **7a** were 21, 14, and 21 h. The intensities were integrated after using a dynamic peak profile analysis, and an estimated mosaic spread (EMS) check[27] was performed to prevent overlapping intensities. A total of 5000 reflections (8000 for **7a**) were selected out of the whole limiting sphere for the cell parameter refinement. A total of 24 515, 21 364, and 12 157 reflections were collected, of which 7385, 5271, and 5953 were unique (R_{int} = 8.66%, 5.73%, and 2.99%) after data reduction. For the numerical absorption correction 11, 12, and 16 indexed crystal faces were used. The structures of **3**, **4**, and **7a** were solved by the Patterson method using an improved version of SHELXS-97[28] and refined with SHELXL-97.[29] For **3** all boron-bonded H atoms were from difference electron density maps. The positional parameters of these atoms could not be refined and were fixed during refinement. The isotropic displacement parameters of the H atoms attached to the crystallographically independent B atoms were refined. The crystals in the batch of **7a** were either twinned or otherwise intergrown, and a block with minimal intergrown parts was selected for the X-ray experiment. The unit cell was determined by using the Stoe IPDS software DISPLAY, XYZ, and RECIPE,[27] omitting weak reflections belonging to intergrown parts. After this procedure the space group could be determined as *Pbca*. It has been assumed that the weak reflections belonged to intergrown parts of other individuals in the crystal and that intensities of the *Pbca* data set contained additional overlapping intensities of similarly oriented domains. A separation of possible twin reflections with RECIPE was not possible. The structure could be solved without problems, and the refinement did not indicate any difficulties. However, inspection of bond distances and angles (Table 6) revealed large deviations and bond ranges: e.g., N(1)−O(2) = 1.304(7) Å. Refinement with soft restraint bond lengths (using fixed average bond lengths with allowance of large shifts) did not change the model geometry significantly.

For compound **6** the data collection was performed at 233-(5) K using a Siemens P3 diffractometer with graphite-monochromated Mo Kα radiation. The ω-scan mode with a reflection scan width of 1.6° and variable scan speeds from 2 to 29°/min were used. A total of 48 reflections were selected for the cell parameter refinement. In all, 6140 reflections were measured, 197 of which were rejected due to a strongly asymmetric peak profile (large differences between left and right background) using the program XDISK of the SHELXTL-Plus package.[30] A total of 5349 reflections were unique. Seven indexed crystal faces were used for a numerical absorption correction with the program HABITUS.[31] The structure of **6** was solved by the Patterson method and refined with CRYSTALS.[32]

Acknowledgment. We thank the University of Zurich and the Swiss National Science Foundation for financial support.

Supporting Information Available: Tables giving optimized geometries and final bonding energies for all calculated molecules and tables of crystal data and structure refinement parameters, atomic coordinates, bond lengths, bond angles, anisotropic displacement parameters, and hydrogen coordinates of **3**, **4**, **6**, and **7a**. This material is available free of charge via the Internet at http://pubs.acs.org.

OM000838V

(22) (a) Baerends, E. J.; Ellis, D. E.; Ros, P. *J. Chem. Phys.* **1973**, *2*, 41. (b) Versluis, L.; Ziegler, T. *J. Chem. Phys.* **1988**, *88*, 322. (c) te Velde, G.; Baerends, E. J. *J. Comput. Phys.* **1992**, *99*, 84. (d) Fonseca Guerra, C.; Snijders, J. G.; te Velde, G.; Baerends, E. J. *Theor. Chem. Acta* **1998**, *99*, 391.

(23) Vosko, S. H.; Wilk, L.; Nusair, M. *Can. J. Phys.* **1980**, *58*, 1200.

(24) Becke, A. *Phys. Rev. A* **1988**, *38*, 3098.

(25) (a) Perdew, J. P. *Phys. Rev. B* **1986**, *33*, 8822. (b) Perdew, J. P. *Phys. Rev. B* **1986**, *34*, 7406.

(26) Ziegler, T.; Tschinke, V.; Baerends, E. J. Snijders, J. G.; Ravenek, W. *J. Phys. Chem*. **1989**, *93*, 3050.

(27) Stoe IPDS software for data collection, cell refinement and data reduction, Version 2.87 and 2.92; Stoe & Cie, Darmstadt, Germany, 1997−1999.

(28) SHELXS-97: Sheldrick, G. M. *Acta Crystallogr.* **1990**, *46A*, 467.

(29) SHELXL-97: Sheldrick, G. M. *Program for the Refinement of Crystal Structures*; University of Göttingen, Göttingen, Germany, 1997.

(30) Siemens SHELXTL Plus, 1994.

(31) Herrendorf, W. HABITUS. Ph.D. Thesis, University of Karlsruhe, 1993.

(32) Watkin, D. J.; Prout, C. K.; Carruthers, J. R.; Betteridge, P. W. CRYSTALS Issue 10; Chemical Crystallography Laboratory, University of Oxford, Oxford, U.K., 1996.